

TECHNICAL REPORT STANDARD PAGE

1. Report No. FHWA/LA.16/16-1TIRE		2. Government Accession No.	3. Recipient's Catalog No.
4. Title and Subtitle Development of Alternative Composite Concrete Bridge Systems for Short and Medium Span Bridges		5. Report Date June 30, 2016	
		6. Performing Organization Code LTRC Project Number: 16-1TIRE State Project Number: DOTLT1000069	
7. Author(s) Fatmir Menkulasi, Ph.D, P.E. Dinesha Kuruppuarachchi		8. Performing Organization Report No.	
9. Performing Organization Name and Address Department of Civil Engineering Louisiana Tech University Ruston, LA, 71272.		10. Work Unit No.	
		11. Contract or Grant No.	
12. Sponsoring Agency Name and Address Louisiana Department of Transportation and Development P.O. Box 94245 Baton Rouge, LA 70804-9245		13. Type of Report and Period Covered Final Report July, 2015-June, 2016	
		14. Sponsoring Agency Code	
15. Supplementary Notes Conducted in Cooperation with the U.S. Department of Transportation, Federal Highway Administration			
16. Abstract A total of four new bridge systems for short and medium span bridges are presented. These bridge systems are lightweight, efficient in flexure and shear and can be used in sites with stringent vertical clearance requirements while being able to accelerate construction by eliminating the need for site installed formwork. The investigated systems consists of adjacent hollow precast concrete beams with and without concrete topping. The proposed configurations are compared with traditional adjacent box beam and decked bulb tee systems for spans that range from 80 ft to 150 ft. Both normal weight and lightweight concrete options are investigated. The comparison is made in terms of span to depth ratios, weight, number of strands, live load deflection and camber. It is demonstrated that the two proposed systems (PS1 and PS2) that feature concrete topping are lighter than the adjacent box beam system for all spans considered. Additionally, PS2 requires fewer strands. The proposed topped systems feature lower camber when compared to the adjacent box beam system. PS2 provides shallower superstructure depths for a given span compared to the adjacent box beam system. While the proposed systems that feature concrete topping (PS3 and PS4) are heavier than the decked bulb tee system, they require a smaller number of strands for a given depth. Additionally, the live load deflection and camber for both PS3 and PS4 is generally less than that for decked bulb tees. PS4 provides shallower superstructure depths for a given span compared to the decked bulb tee system. PS2 and PS4 appear to be more competitive than PS1 and PS3. Live load distribution factors (LLDF), for PS1/PS2 and PS3/PS4 can be conservatively estimated using AASHTO provisions for adjacent box and decked bulb tee systems, respectively. Also, LLDF for adjacent box and decked bulb tee systems computed from finite element analysis were lower than those calculated based on AASHTO provisions.			
17. Key Words Short and medium span bridges; composite concrete bridges; shallow superstructure depth; precast beams		18. Distribution Statement Unrestricted. This document is available through the National Technical Information Service, Springfield, VA 21161.	
19. Security Classif. (of this report) N/A	20. Security Classif. (of this page) N/A	21. No. of Pages 69	22. Price N/A

Project Review Committee

Each research project will have an advisory committee appointed by the LTRC Director. The Project Review Committee is responsible for assisting the LTRC Administrator or Manager in the development of acceptable research problem statements, requests for proposals, review of research proposals, oversight of approved research projects, and implementation of findings.

LTRC appreciates the dedication of the following Project Review Committee Members in guiding this research study to fruition.

LTRC Administrator/ Manager

Vijaya Gopu, Ph.D, P.E.

Associate Director

Directorate Implementation Sponsor

Richard Savoie, P.E.

DOTD Chief Engineer

Development of Alternative Composite Concrete Bridge Systems for Short and Medium Span Bridges

by
Fatmir Menkulasi, Ph.D, P.E.
Dinesha Kuruppuarachchi

Department of Civil Engineering
Louisiana Tech University
Ruston, LA 71272.

LTRC Project No. 16-1TIRE
State Project No. DOT-LT-1000069

conducted for

Louisiana Department of Transportation and Development
Louisiana Transportation Research Center

The contents of this report reflect the views of the author/principal investigator who is responsible for the facts and the accuracy of the data presented herein. The contents of this report do not necessarily reflect the views or policies of the Louisiana Department of Transportation and Development, the Federal Highway Administration, or the Louisiana Transportation Research Center. This report does not constitute a standard, specification, or regulation.

June, 2016

ABSTRACT

A total of four new bridge systems for short and medium span bridges are presented. These bridge systems are lightweight, efficient in flexure and shear and can be used in sites with stringent vertical clearance requirements while being able to accelerate construction by eliminating the need for site installed formwork. The investigated systems consists of adjacent hollow precast concrete beams with and without concrete topping. The proposed configurations are compared with traditional adjacent box beam and decked bulb tee systems for spans that range from 80 ft to 150 ft. Both normal weight and lightweight concrete options are investigated. The comparison is made in terms of span to depth ratios, weight, number of strands, live load deflection and camber. It is demonstrated that the two proposed systems (PS1 and PS2) that feature concrete topping are lighter than the adjacent box beam system for all spans considered. Additionally, PS2 requires fewer strands. The proposed topped systems feature lower camber when compared to the adjacent box beam system. PS2 provides shallower superstructure depths for a given span compared to the adjacent box beam system. While the proposed systems that feature concrete topping (PS3 and PS4) are heavier than the decked bulb tee system, they require a smaller number of strands for a given depth. Additionally, the live load deflection and camber for both PS3 and PS4 is generally less than that for decked bulb tees. PS4 provides shallower superstructure depths for a given span compared to the decked bulb tee system. PS2 and PS4 appear to be more competitive than PS1 and PS3. Live load distribution factors (LLDF), for PS1/PS2 and PS3/PS4 can be conservatively estimated using AASHTO provisions for adjacent box and decked bulb tee systems, respectively. Also, LLDF for adjacent box and decked bulb tee systems computed from finite element analysis were lower than those calculated based on AASHTO provisions.

ACKNOWLEDGMENTS

The investigators are grateful to the Louisiana Transportation Research Center (LTRC) and Louisiana Department of Transportation and Development (LADOTD) for funding this project.

IMPLEMENTATION STATEMENT

The composite concrete bridge superstructures developed as part of this study can be used in the construction of short and medium span bridges with spans ranging from 80 ft to 150 ft. The proposed method of construction features adjacent precast elements, which serve as stay-in-place formwork for the cast-in-place components and eliminate the need for site installed formwork. This approach accelerates the construction of new bridges and rehabilitation of existing ones. The proposed bridge systems are ideal for sites with stringent vertical clearance requirements where the overall depth of the superstructure is limited. The developed live load distribution factors can be used in the design of the proposed bridge systems using a traditional beam line analysis. The recommendations related to the longitudinal connections between the adjacent precast members can be used in the design and detailing of these connections.

TABLE OF CONTENTS

ABSTRACT.....	v
ACKNOWLEDGMENTS	vi
IMPLEMENTATION STATEMENT	vii
TABLE OF CONTENTS.....	ix
LIST OF TABLES	xi
LIST OF FIGURES	xiii
INTRODUCTION	1
OBJECTIVE	3
SCOPE	5
METHODOLOGY	7
Description of the Proposed Bridge Systems.....	8
Live Load Distribution Factors	12
Design of Superstructure Systems	18
Longitudinal Connections.....	20
DISCUSSION OF RESULTS	27
Live Load Distribution Factors	27
Design of Superstructure Systems	30
Validation.....	30
Topped Systems	30
Un-topped Systems	41
Longitudinal Connections.....	52
Topped Systems	52
Un-topped Systems	60
CONCLUSIONS.....	66
ACRONYMS, ABBREVIATIONS, AND SYMBOLS	68
REFERENCES	69

LIST OF TABLES

Table 1 Summary of bridge configurations included in the comparison study	12
Table 2 Comparison of number of strands using various design tools (Box beams -NW)	30
Table 3 Comparison of number of strands using various design tools (DBT - NW)	30
Table 4 Controlling parameters for the normal weight concrete option (topped systems).....	33
Table 5 Controlling parameters for the lightweight concrete option (topped systems).....	33
Table 6 Design of precast concrete SIP forms.....	34
Table 7 Design of composite deck.....	34
Table 8 Materials use comparison (normal weight)	36
Table 9 Materials use comparison (light weight)	37
Table 10 Summary of live load deflection and camber values	39
Table 11 Superstructure depths for Box system	39
Table 12 Weight and number of strands for PS2 and shallowest Box.....	40
Table 13 Number of strands required for PS2 system for shallower superstructure depths...	41
Table 14 Controlling parameters (normal weight concrete) (un-topped systems)	44
Table 15 Controlling parameters (lightweight concrete) (un-topped systems)	45
Table 16 Top flange design for un-topped systems	46
Table 17 Materials use comparison (normal weight)	48
Table 18 Materials use comparison (lightweight)	48
Table 19 Live load deflections and camber for un-topped systems.....	50
Table 20 Superstructure depths for DBT system.....	51
Table 21 Number of strands for PS4 and shallowest DBT.....	52
Table 22 Number of strands required for PS4 system for shallower superstructure depths...	52
Table 23 Transverse tensile forces in PS1	53
Table 24 Transverse tensile forces in PS2	53
Table 25 Test matrix for beam splice tests (adapted from Halbe [15])	55
Table 26 Results of beam splice tests with 2-No.4 tension bars (adapted from Halbe [15]).	56
Table 27 Results of beam splice tests with 2-No.6 tension bars (adapted from Halbe [15]).	56
Table 28 Test matrix for specimens tested during Phase I (Menkulasi [16]).....	59
Table 29 Test results for specimens tested by Menkulasi [16]	60
Table 30 Transverse bending moment in PS3	62
Table 31 Transverse bending moment in PS4	62
Table 32 Transverse bending moment in DBT.....	62
Table 33 Closure pour materials used by French et al. [7].....	65
Table 34 Tested concrete compressive strengths (French et al. [7])	65
Table 35 Measured panel moment capacities (French et al. [7])	65

LIST OF FIGURES

Figure 1 Proposed Bridge Systems	8
Figure 2 Transverse cross-section of the proposed systems	9
Figure 3 Transverse cross-section of traditional systems	10
Figure 4 C-grid.....	11
Figure 5 Finite element mesh for all investigated systems	14
Figure 6 Truck and tandem load positions used for determining LLDFs for moment	16
Figure 7 Truck and tandem load positions used for determining LLDFs for shear.....	16
Figure 8 Illustration of approach for computing LLDFs (U_2 = vertical deflection, units = in.)	17
Figure 9 Longitudinal connections for topped systems	22
Figure 10 Calculation of transverse tensile force in proposed topped systems	23
Figure 11 Longitudinal connection for un-topped system.....	24
Figure 12 Calculation of transverse bending moment in un-topped systems	25
Figure 13 Comparison of LLDFs for moment.....	28
Figure 14 Comparison of LLDFs for shear.....	28
Figure 15 LLDF for moment in each beam for the 80 ft span.....	29
Figure 16 Mesh sensitivity analysis (LLDF _m for DBT 80 ft span).....	29
Figure 17 Strand configuration for Box beams.....	31
Figure 18 Strand Configuration for PS1	32
Figure 19 Strand configuration PS2.....	32
Figure 20 Composite and non-composite weights of individual precast beams (topped systems).....	35
Figure 21 Number of strands per 6 ft of width (topped systems)	36
Figure 22 Live load deflection and camber comparison (topped systems)	38
Figure 23 Strand Configuration for Decked Bulb Tees	42
Figure 24 Strand configuration for PS3	43
Figure 25 Strand configuration for PS4	44
Figure 26 Material comparison between PS3, PS4 and DBT	47
Figure 27 Number of strands comparison.....	47
Figure 28 Live load deflection and camber comparison (un-topped system).....	50
Figure 29 Test setup for beam splice tests (reprinted from Halbe [15]).....	54
Figure 30 Splice detail and force diagram (reprinted from Halbe [15]).....	54
Figure 31 Partial transverse cross-section of the bridge system developed by Menkulasi [16]	57
Figure 32 Welded connection tested by Menkulasi [16].....	58

Figure 33 Test setup used by Menkulasi [16]	58
Figure 34 Tested specimens with welded connections (Menkulasi [16])	58
Figure 35 Strut and tie model (Menkulasi [16]).....	59
Figure 36 Tested slab dimensions and shear key details (French et al. [7]).....	64
Figure 37 Joint reinforcing details (French et al. [7])	64

INTRODUCTION

Bridges superstructures with shallow overall depth are in high demand in sites with stringent vertical clearance requirements. Examples include bridges built over existing highways, or bridges crossing various bodies of water. The traditional bridge systems used in these situations include adjacent box structures and decked bulb tees. Adjacent box structures are efficient because they utilize the strength and stiffness of several structural components placed in closed proximity to one another. They also provide a working platform for placing a concrete topping or other types of overlay, which are needed to provide a smooth riding surface. However, adjacent box structure systems have exhibited problems related to reflective cracking, which occurs as a result of the failure of the connection between the adjacent precast members. The female-to-female type of shear keys traditionally used in these systems may provide an efficient mechanism in resisting shear forces, but when the keyed joint is subject to transverse bending moments, the only resisting mechanism is primarily the tensile bond between the grout in the shear key and the precast concrete. Transverse post-tensioning helps in resisting transverse bending moment but is an operation that needs to be carried out in the field and works against the concept of accelerating bridge construction [1].

Huckelbridge et al. conducted several field tests on box girder bridges to investigate the performance of the shear keys and concluded that all bridges tested exhibited relative displacements across at least some of the joints, which indicated a fractured shear key [2]. Miller et al. conducted several full scale tests of shear keys between adjacent box beams and concluded that thermal stresses sometimes caused cracking in the shear keys before any loading was applied [3]. Additionally, details in which the shear key was closer to the neutral axis performed better than those in which the shear key was closer to the top surface. One of the causes that can lead to reflective cracking is the transverse bending of the bridge when subject to concentrated loads such as vehicular loads. El-Remaily et al., Badwan and Liang, and Hanna et al. proposed grillage methods of analysis to quantify the amount of post-tensioning needed to address reflective cracking problems due to the transverse bending of the bridge [4], [5], [6]. Additionally, several parametric studies were conducted to investigate the influence of various parameters on the required amount of transverse post-tensioning such as: bridge width, beam depth, span-to-depth ratio and skew angle. As stated earlier, while transverse post-tensioning helps reduce tensile stresses in the shear keys caused by transverse bending of the bridge, it also works against the concept of accelerating bridge construction and requires specialty contractors.

Decked bulb tees is another superstructure system that features adjacent precast members ideal for sites with stringent vertical clearance requirements. Research by French et al. shows that doweled connections filled with site cast concrete are capable of emulating monolithic action and in resting design level forces [7]. From a stability perspective the decked bulb tee system benefits from the placement of end or intermediate diaphragms such that work related to longitudinal connections can be performed on a more stable platform.

The goal of this project is to develop alternative composite concrete bridge systems for short to medium-span bridges, which are lightweight, efficient in flexure and shear and can be used in sites with stringent vertical clearance requirements while being able to accelerate construction by eliminating the need for site installed formwork. The investigated systems consists of adjacent hollow precast concrete beams with and without concrete topping. A total of four new bridge systems are investigated. The proposed configurations are compared with traditional adjacent box beam and decked bulb tee systems for spans that range from 80 ft to 150 ft. In the systems that feature a concrete topping the location of the longitudinal connection between adjacent precast members is shifted towards the bottom such that a tension tie is created to resist transverse bending moments. This is intended to emulate monolithic action without the need for transverse post-tensioning. The systems that feature no topping have longitudinal connections similar to those used in decked bulb tees, and feature a configuration that provides a stable working platform for performing the work related to connections. Additionally, in the proposed un-topped systems transverse bending moment demands on the longitudinal connections and on the top precast flange are reduced due to the reduced span provided by the two web supports as opposed to the single web support in the decked bulb tee system.

OBJECTIVE

The goal of this project is to develop alternative composite concrete bridge systems for short to medium-span bridges, which are lightweight, efficient in flexure and shear and can be used in sites with stringent vertical clearance requirements while being able to accelerate construction by eliminating the need for site installed formwork.

SCOPE

A total of four new composite concrete bridge systems are investigated. The proposed configurations are compared with traditional adjacent box beam and decked bulb tee systems for spans that range from 80 ft to 150 ft. Both normal weight and light weight concrete options are investigated. The comparison is made in terms of span to depth ratios, weight, live load deflection and camber. To be consistent in the comparison with the traditional systems, live load distribution factors (LLDFs) for all systems are calculated using 3D finite element analyses (FEA). The design of transverse connections is a unique feature in the proposed bridge systems. As a result, to facilitate the design of these connections, the tensile forces and bending moments that these connections are subject to are tabulated.

METHODOLOGY

A total of four bridge superstructure systems are proposed for use in short and medium span bridges with spans ranging from 80 ft to 150 ft. The investigated systems consist of adjacent hollow precast concrete beams with and without topping. The proposed bridge systems are compared with traditional adjacent box and decked bulb tee systems in terms of span to depth ratios, weight, number of strands, live load deflection and camber. To be consistent in the comparison with traditional systems, live load distribution factors (LLDFs) for all systems are calculated using 3D finite element analysis. These live load distribution systems are then used in the structural design of the bridge superstructure for gravitational loads. The analysis and design of the bridge superstructures is performed based on AASHTO LFRD Specifications using a combination of mathematical and analysis softwares such as Mathcad, Conspan and Abaqus [8], [9], [10], [11]. Flexural stress, flexural strength, shear strength and deflection checks are implemented to ensure that the proposed bridge systems work.

For each span length the depth of the superstructure for the traditional systems was chosen using the design aids in the PCI Bridge Design Manual [12]. The superstructure depth for the proposed systems was kept the same so that a comparison could be made in terms of weight, number of strands, live load deflection and camber.

The next step was to determine how much shallower could the superstructure depth be for the traditional systems if LLDFs for moment computed from FEA were used instead of those calculated based on AASHTO LFRD Specifications [8]. This information will be useful in determining how big of a benefit does a more accurate computation of live load distribution factors provide in terms of supplying a shallower superstructure depth. Once the shallowest superstructure depth for the traditional systems was obtained, the proposed systems were designed to maintain the same depth and a comparison in terms of weight and the number of strands required was performed.

The final exercise in terms of comparison was to determine whether the proposed systems could supply a shallower superstructure depth compared to the absolute minimum obtained for the traditional systems. The superstructure depth for the proposed systems was made 2 in. shallower than the absolute minimum for the traditional systems and the required number of strands was determined. It was outside the scope of work to determine the absolute minimum superstructure depth for a given span for the proposed systems because the main goal was to demonstrate that the proposed systems are competitive with the traditional systems. Because all proposed systems feature either discrete or continuous transverse connections

along the longitudinal joints between adjacent precast members, it is important to quantify the forces that these connections will be subject to. As a result, tension forces and bending moments created due to the transverse bending of the bridge were quantified and tabulated so that they can be used in the design of these connections.

Description of the Proposed Bridge Systems

Figure 1 provides 3D renderings of the proposed bridge systems and Figure 2 provides transverse cross-sections. Two of the proposed systems (PS1 and PS2) feature concrete topping (topped systems) and the other two (PS3 and PS4) feature no topping (un-topped systems). The individual precast beams for each system are magnified in Figure 1 so that they can be better illustrated. The first proposed system (PS1) features adjacent hollow trapezoidal precast beams with the larger base at the bottom. The second proposed system (PS2) is similar with the exception that the webs are straight as opposed to tapered. The third and fourth proposed systems (PS3 and PS4) feature similar precast shapes with the exception that the larger base is provided at the top to eliminate the need for a concrete topping.

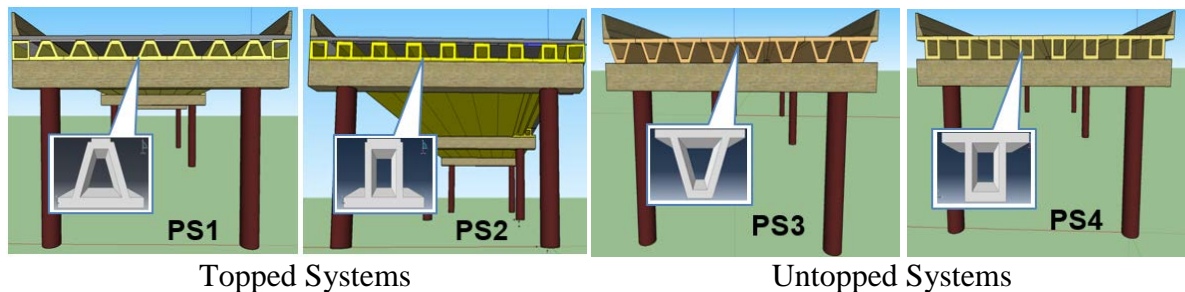
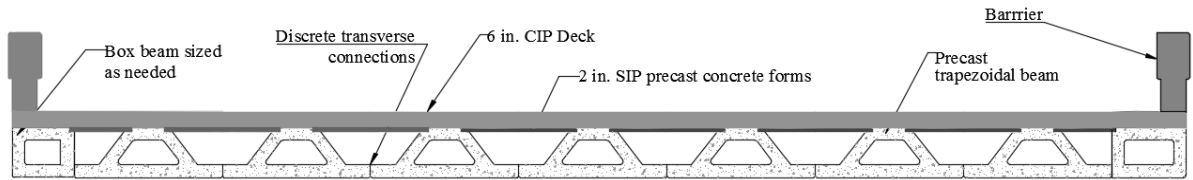
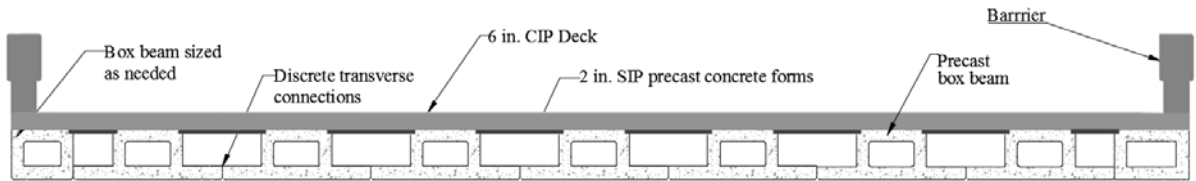


Figure 1
Proposed Bridge Systems

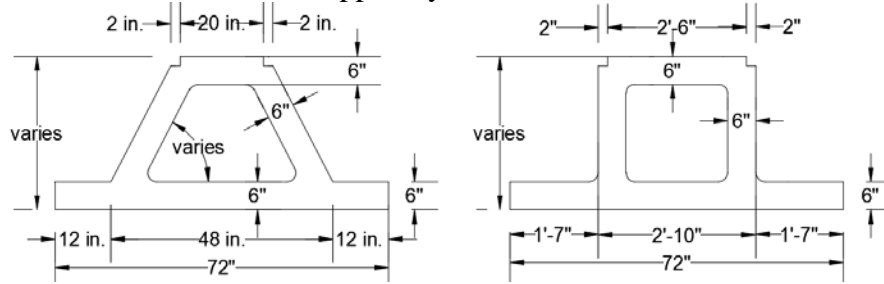
PS1 and PS2 are compared with the traditional adjacent box beam system (Figure 3) because they feature concrete topping, and PS3 and PS4 are compared with the traditional decked bulbed tee system (Figure 3) provided that they feature no topping. The width of all bridges is 48 ft and they are considered to represent 3 lane bridges. The width of the individual precast beams in the proposed systems is 6 ft. Customized edge box beams are provided to support the barrier and the edge of the concrete topping. The un-topped systems do not need any customized edge members and the barrier is supported on the top flange of the precast trapezoidal beams.



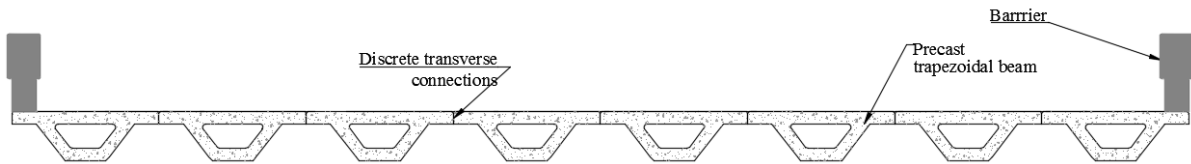
Topped System – PS1



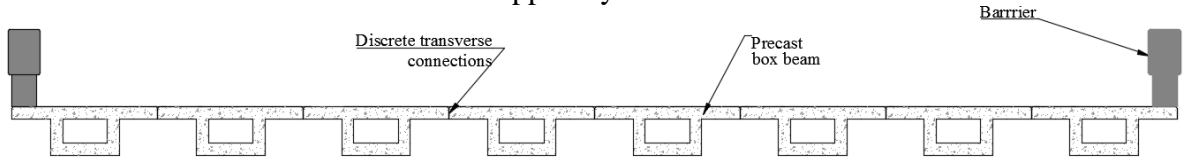
Topped System – PS2



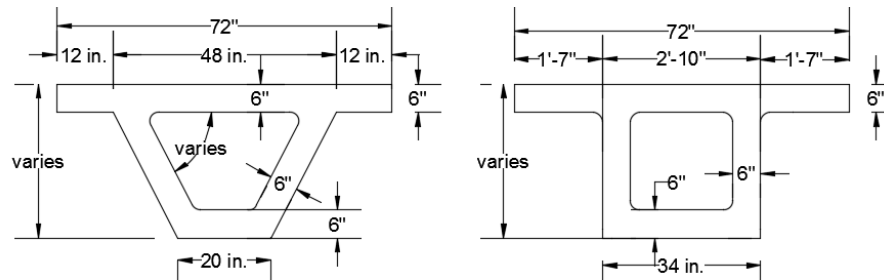
Typical precast beam dimensions for the topped systems



Un-topped System – PS3

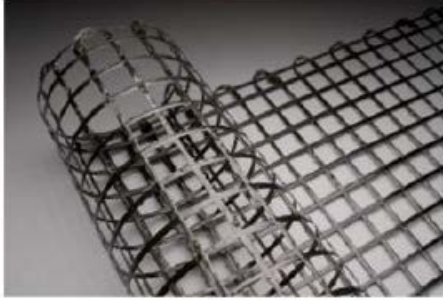


Un-topped System – PS4



Typical precast beam dimensions for the un-topped systems

Figure 2
Transverse cross-section of the proposed systems



C-grid (Source: www.chomarat.com) [13]

Figure 4
C-grid

Three span lengths are considered for the topped systems, 80 ft, 100 ft, and 120 ft, respectively. Four span lengths are considered for the un-topped systems, 80 ft, 100 ft, 120 ft, and 150 ft. Both normal weight and light weight options are investigated. The unit weight of normal weight and lightweight concrete was assumed to be 150 pcf, and 120 pcf, respectively, for weight estimation purposes. The concrete design compressive strength at 28 days for the precast beams and CIP topping was assumed to be 8000 psi, and 4000 psi, respectively. The concrete design compressive strength at 28 days for the precast SIP forms was assumed to be 4000 psi. The moduli of elasticity for all components were calculated based on AASHTO using a unit weight of 145 pcf for normal weight concrete and 115 pcf for lightweight concrete [8]. Poisson's ratio was taken equal to 0.2 and it was used during finite element analyses.

All prestressing strands are 0.6 in. diameter low relaxation strands grade 270 ksi. The modulus of elasticity for the prestressing strands was taken equal to 28500 ksi. The weight of the barriers was assumed to be 0.25 k/ft for each barrier and the unit weight for the future wearing surface was taken equal to 140 pcf. The thickness of the future wearing surface was taken equal to 3 in. Table 1 provides a summary of all bridge configurations and some of the assumptions used in this study.

Table 1
Summary of bridge configurations included in the comparison study

Span (ft)	Type	Depth (in.)	Notes
80	Adjacent box beam (BII – 48)	33	<u>Concrete Unit Weight</u> Normal weight = 150 pcf, Lightweight = 120 pcf <u>Configuration</u> Single Span, Bridge width = 48 ft <u>Materials -Concrete</u> Precast beams, $f'_c = 8000$ psi, CIP topping, $f'_c = 4000$ psi Precast SIP forms $f'_c = 4000$ psi E = based on AASHTO, $\nu = 0.2$ <u>Materials – Steel</u> $f_y = 60$ ksi (typ.), $f_y = 75$ ksi deformed wire <u>Materials –Strands</u> Diameter = 0.6 in. Type = low relaxation Grade, $f_{pu} = 270$ ksi E = 28500 ksi <u>Materials – C-grid</u> C50 – 1.8x1.6, E = 34,000 ksi, $\epsilon_{ult} = 0.0099$ $A_{transverse} = 0.021450$ in ² /ft, $A_{longitudinal} = 0.019067$ in ² /ft, Linear elastic <u>Barrier and future wearing surface (FWS)</u> Barrier _{weight} = 0.25 k/ft, FWS _{weight} = 140 pcf
	Deck Bulb Tee (BT-35)	35	
	PS1	33	
	PS2	33	
	PS3	35	
	PS4	35	
100	Adjacent box beam (BIII - 48)	39	
	Deck Bulb Tee (BT-41)	41	
	PS1	39	
	PS2	39	
	PS3	41	
	PS4	41	
120	Adjacent box beam (BIV – 48)	42	
	Deck Bulb Tee (BT-53)	53	
	PS1	42	
	PS2	42	
	PS3	53	
	PS4	53	
150	Deck Bulb Tee (BT – 65)	65	
	PS3	65	
	PS4	65	

The proposed systems are intended to provide competitive alternatives with the traditional systems in terms of structural efficiency and construction time. The topped system will take longer to construct compared to the un-topped systems because of the presence of the CIP concrete topping, however no joints will be exposed to traffic. The un-topped systems offer a more attractive alternative from the perspective of accelerating construction, however the longitudinal joints between the adjacent members will be exposed to traffic.

Live Load Distribution Factors

Live load distribution factors (LLDFs) for all proposed bridge systems were computed using the commercially available finite element analysis software Abaqus [11]. To be consistent in the comparison with traditional systems, LLDFs for traditional systems were also computed using finite element analyses. All computations related to LLDFs were based on the single span three lane bridge configurations described earlier.

3D solid elements with incompatible modes (C3D8I) were used in all numerical simulations. Figure 5 shows the finite element mesh for all investigated systems. The 3D solid elements with incompatible modes are first-order elements that are enhanced by incompatible modes to improve their bending behavior. In addition to the standard displacement degrees of freedom, incompatible deformation modes are added internally to the elements [11]. The primary effect of these modes is to eliminate the parasitic shear stresses that cause the response of the regular first-order displacement elements to be too stiff in bending [11]. In addition, these modes eliminate the artificial stiffening due to Poisson's effect in bending (which is manifested in regular displacement elements by a linear variation of the stress perpendicular to the bending direction) [11]. In regular displacement elements the linear variation of the axial stress due to bending is accompanied by a linear variation of the stress perpendicular to the bending direction, which leads to incorrect stresses and an overestimation of the stiffness. The incompatible modes prevent such a stress from occurring [11]. Because of the added internal degrees of freedom due to the incompatible modes these elements are somewhat more expensive than the regular first-order displacement elements; however, they are significantly more economical than second-order elements [11]. The incompatible mode elements use full integration and, thus, have no hourglass modes [11]. The shape of the elements was tried to be kept as rectangular or as square as possible, however, in cases that featured inclined webs or tapered flanges, the solid elements featured parallelogram or trapezoidal shapes. A mesh sensitivity analysis was conducted to ensure that the selected size of the mesh did not influence the magnitude of LLDFs.

All numerical simulations were linear elastic because the all investigated systems were fully prestressed and tensile stresses did not exceed allowable ones. Additionally, it was ensured that the maximum tensile stress in the transverse direction due to live loads did not exceed the tensile strength of concrete.

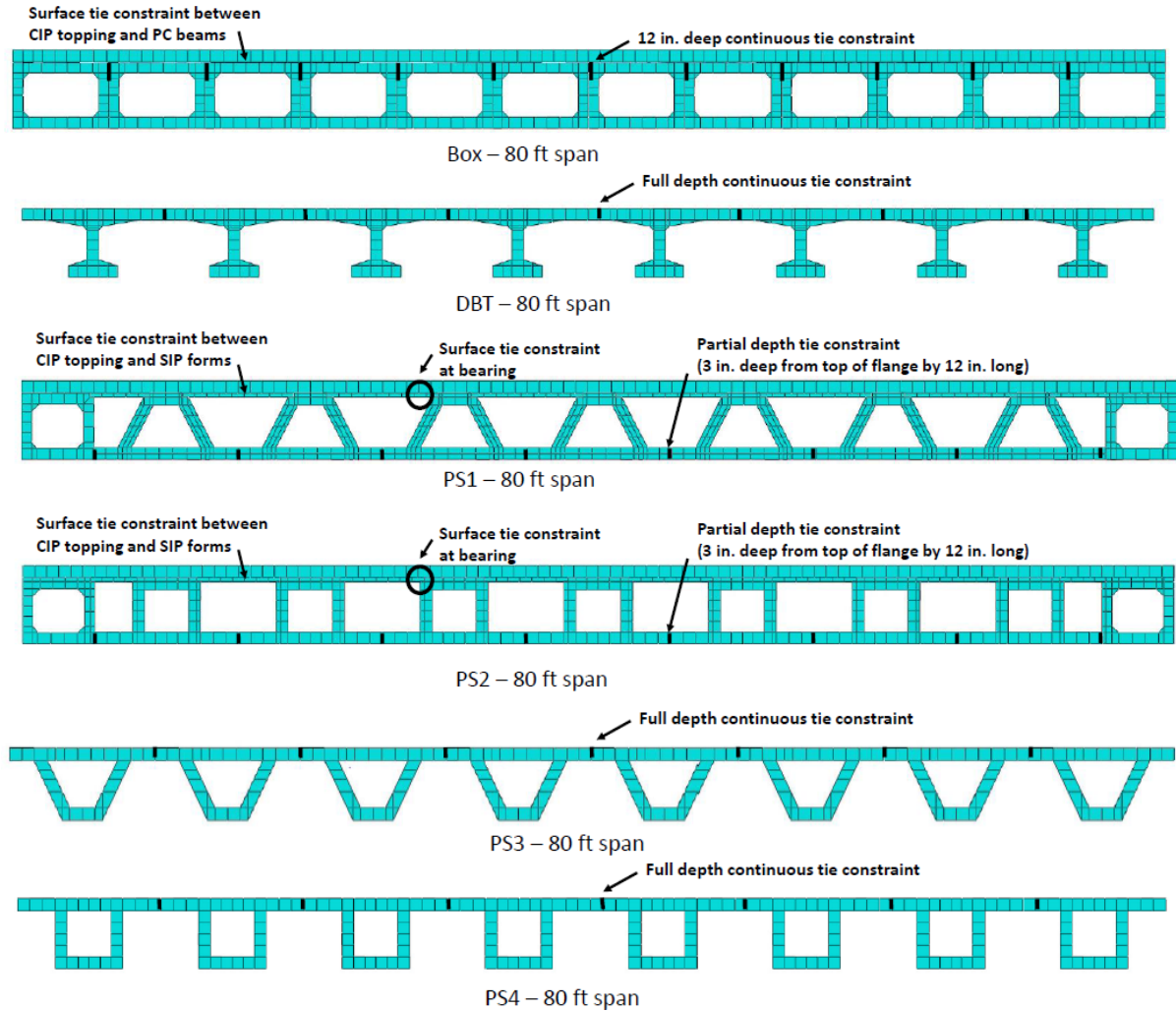


Figure 5
Finite element mesh for all investigated systems

LLDFs were calculated by considering combinations of truck plus lane and tandem plus lane loading. The loading cases in the transverse direction of the bridge included one, two, and three truck/tandem configurations. Additionally, in the transverse direction the truck and tandem loading was varied such that it was positioned as close to the edge of the barriers as AASHTO allows as well as at mid-width of the bridge to identify the worst case scenario. Figure 6 illustrates the live load positions investigated to determine the highest LLDFs for moment, whereas Figure 7 illustrates the live load positions investigated to determine the highest LLDFs for shear. Although both cases with and without a barrier were considered, only LLDFs for cases that featured no barrier are reported because the presence of a continuous structural barrier cannot be always relied upon.

Equation 1 was used to calculate LLDFs for moment. In the longitudinal direction, the truck/tandem configurations were positioned at mid-span. The LLDF for moment for each beam was calculated by dividing the product of the deflection at mid-span of the beam, modulus of elasticity and moment of inertia, by the sum of products representing all beams. Deflections were obtained at mid-width of each beam. Figure 8 shows the transverse bending of the bridge superstructure due to design live loads and the approach for computing LLDFs for moment using deflections at mid-span and mid-width of each beam. LLDFs for shear for each beam were calculated by dividing the reaction at each beam with the sum of reactions from all beams (Equation 2). In the longitudinal direction, the truck/tandem configurations were positioned at a distance d from the face of the support.

After LLDFs for each beam were calculated, the maximum value was considered to represent the LLDF for that particular load case. The probability of multiple trucks being present at the same time was taken into account by using the multiple presence factors provided in AASHTO. The computed LLDFs were compared with those predicted based on AASHTO's equations assuming adjacent box structure and decked bulb tee behavior, for topped and untopped systems, respectively.

$$LLDF_i = \frac{\Delta_i E_i I_i}{\sum_{i=1}^6 \Delta_i E_i I_i} * multiple\ presence\ factor * No.\ of\ trucks \quad (1)$$

where,

Δ_i = Deflection at mid-width and mid-span of each beam

$LLDF_i$ = Live load distribution factor for each beam

$$LLDF_i = \frac{R_i}{\sum_{i=1}^6 R_i} * multiple\ presence\ factor * No.\ of\ trucks \quad (2)$$

where,

R_i = Vertical reaction at each beam

$LLDF_i$ = Live load distribution factor for each beam

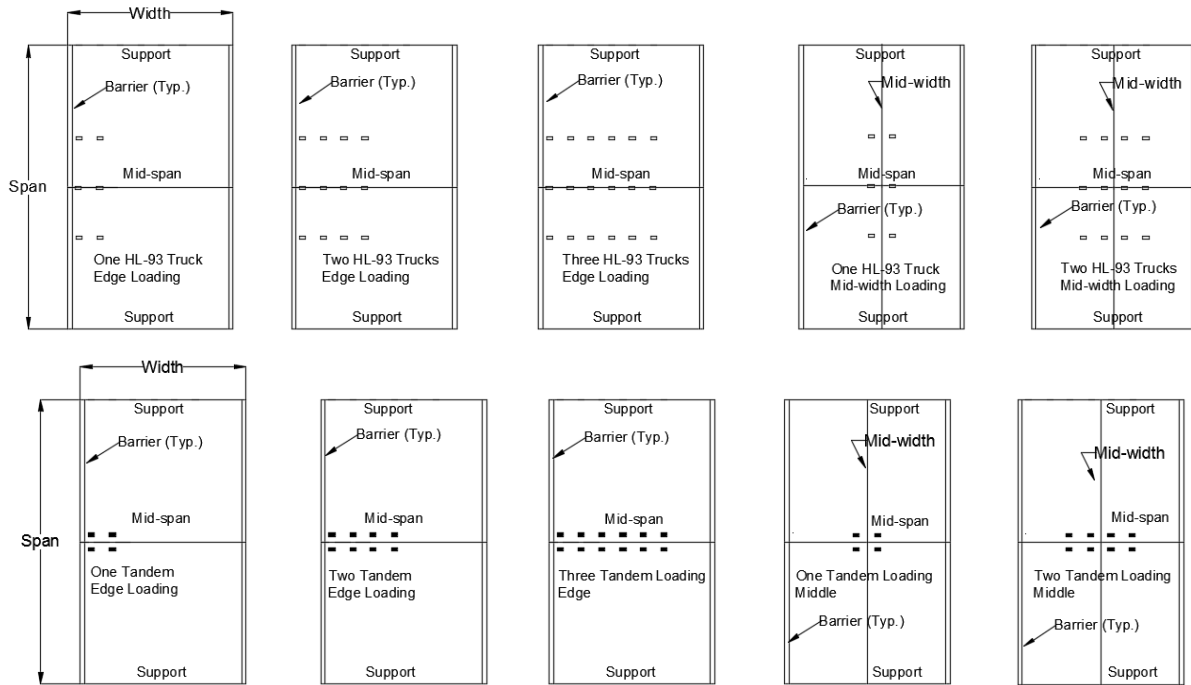


Figure 6
Truck and tandem load positions used for determining LLDFs for moment

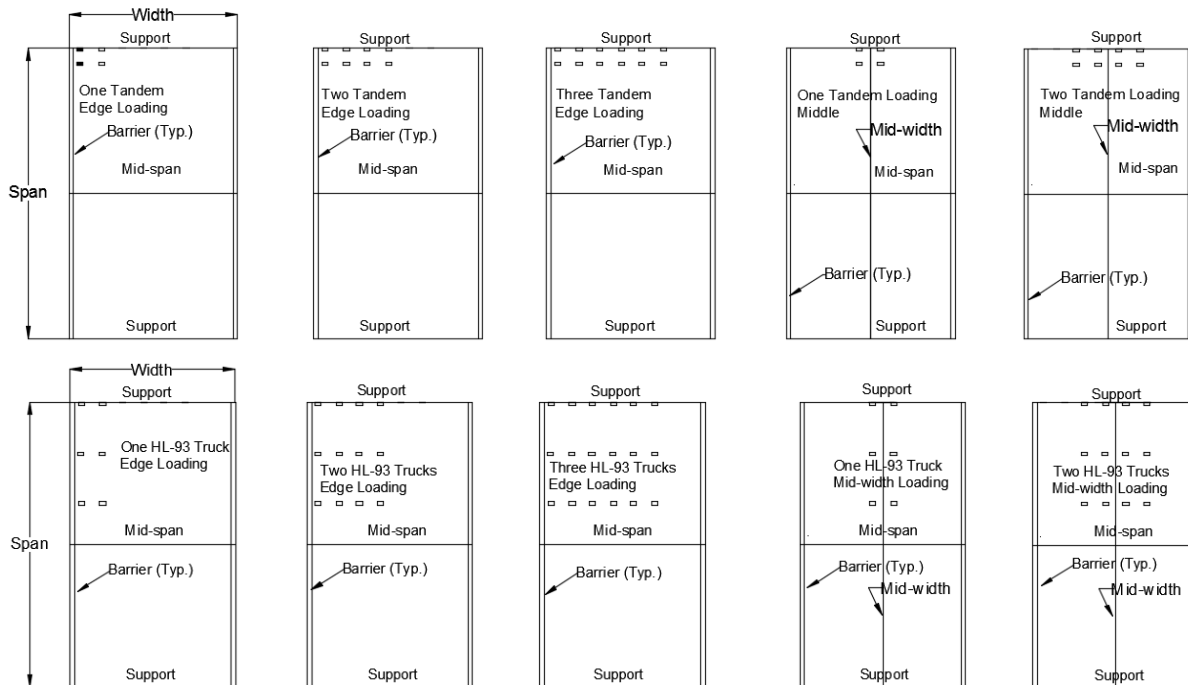
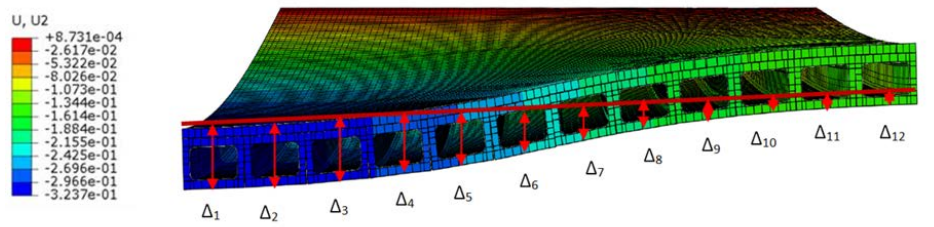
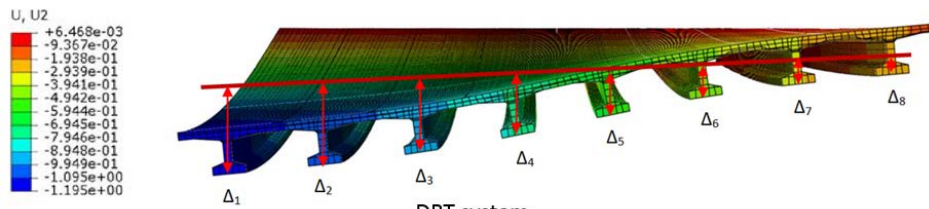


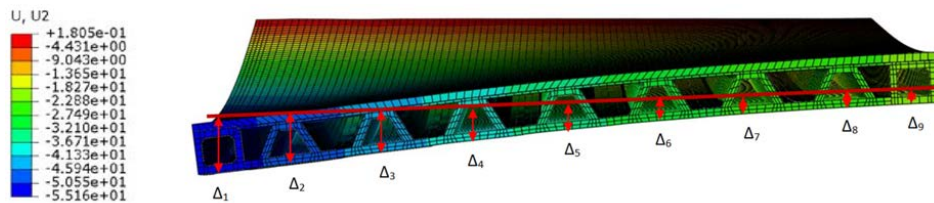
Figure 7
Truck and tandem load positions used for determining LLDFs for shear



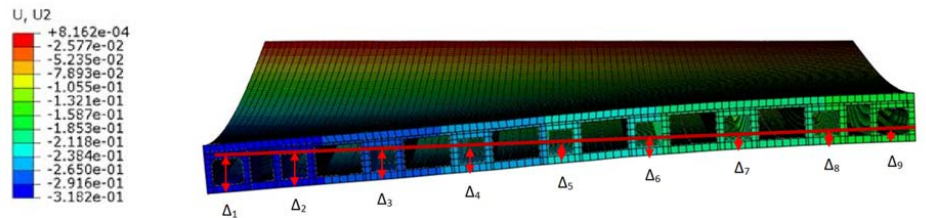
Adjacent Box Beam System



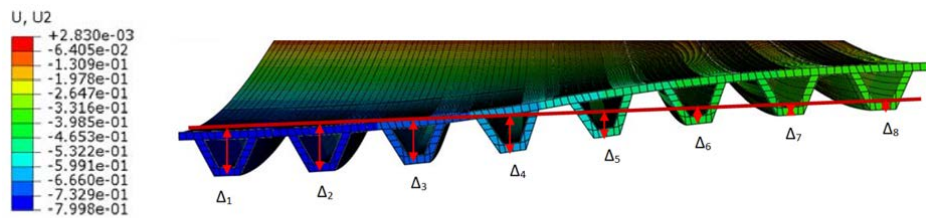
DBT system



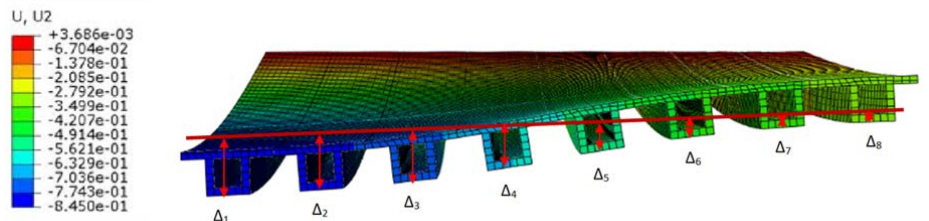
PS1 – topped system



PS2 – topped system



PS3 – un-topped system



PS4 beam – un-topped system

Figure 8
Illustration of approach for computing LLDFs (U2 = vertical deflection, units = in.)

For the topped systems the bond between the precast beams and cast-in-place topping was assumed to be a perfect bond. This is a reasonable assumption because due to the large contact surface between the precast and CIP components, interface shear stresses are rather small. Additionally, a 12 in deep shear key was assumed for the traditional adjacent box beam system. To simulate the presence of the shear key, the adjacent box beams were connected using a tie constraint for the 12 in. depth of the shear key measured from the top of the box beam. This implies that the shear key will not fail and serve as intended when subject to design loads. The connection between the flanges of adjacent decked bulb tees was simulated using a continuous tie constraint for the full depth of the flange. Again, this means that the actual connection will behave as intended and that it will not fail when subject to design loads. The same assumption was used for PS3 and PS4. The connection between the SIP forms and CIP topping and the SIP forms and precast beams was modeled as a perfect bond. Again, this is a reasonable assumption because of the large contact surface between these components.

Design of Superstructure Systems

All proposed and traditional systems were designed based on AASHTO LFRD Specifications using Mathcad [8], [9]. For each span length the depth of the superstructure for the traditional systems was chosen using the design aids in the PCI Bridge Design Manual [12]. The superstructure depth for the proposed systems was kept the same so that a comparison could be made in terms of weight, number of strands, live load deflection and camber. The number of strands obtained from Mathcad calculations for the traditional bridge systems was compared with that obtained from the PCI Bridge Design Manual and Conspan software to validate the approach [12], [10]. For the traditional systems and for the proposed systems that featured straight webs a portion of the strands were harped to control tensile stresses at the ends. For the proposed systems that featured tapered webs all prestressing strands were straight.

The comparison between the proposed systems and the traditional systems was performed in terms of material use, live load deflection and camber. In terms of materials use, composite and non-composite weights of typical repetitive sections in the traditional systems were compared with those of the proposed systems. Additionally, the number of strands used in each system was compared. The stiffness of each systems was expressed in terms of live load deflections and camber. Deflections and camber were conservatively calculated using gross cross-sectional properties rather than the un-cracked transformed cross-sectional properties. There are generally two design approaches for calculating deflections. The first one is to conduct a beam line analysis for the design live loads and multiply the maximum deflection

by the ratio of design lanes divided by the total number of beams. The second is to multiply the maximum deflection obtained from the beam line analysis for the design live loads with the LLDF for moment. The PCI Bridge Design Manual states that it is more conservative to follow the second approach when calculating live load deflections. The first assumption assumes a certain degree of continuity between the adjacent members and does not distinguish from one type of superstructure to the next. The LLDF for moment approach distinguishes the continuity present in the transverse direction from one superstructure to the next in terms of LLDFs. As a result, the second approach was followed for calculating the live load deflections reported herein.

The SIP forms for the proposed topped systems were designed to support their self-weight, the weight of the wet concrete topping, and 20 psf construction loads without incurring any cracking at service. Additionally, the topping and the SIP forms were designed compositely to support any superimposed live loads without incurring any cracking at service. A moving load analysis was performed to obtain worst case positive and negative moments at service and at ultimate.

AASHTO's strip method was used to determine the effective width that can be used when estimating moment capacities. At the ultimate limit state the composite deck was designed by taking into account the presence of the C-grid and reinforcing steel when estimating the nominal flexural strength. The diameter of the C-grid is 0.06 in. and the spacing of the grid is 1.6 in. in the transverse direction and 1.8 in. in the longitudinal direction (C50-1.8x1.6). The C in the C50 designation indicates carbon fibers and the 50 indicates the relative size of the strand. For example, C100 has approximately twice the cross-sectional area of C50 strands. The C-grid is typically supplied in widths of 47.5 in. or 95 in. [13]. The modulus of elasticity for the C-grid was taken equal to 34,000 ksi and the ultimate strain was taken equal to $\epsilon_{ult} = 0.0099$. The stress strain relationship for the C-grid was assumed to be linear elastic. The area of carbon fiber strands per unit width was 0.021450 in²/ft in the transverse direction and 0.019067 in²/ft in the longitudinal direction. Both proposed topped systems require only one layer of C-grid. The design compressive strength for the concrete is $f'_c = 4,000$ psi. The reinforcing in the CIP topping for PS1 and PS2 was assumed to be No.4 at 12 in. on center in each direction.

The top flange of the un-topped systems was designed for live loads in the transverse direction using AASHTO's strip method. A moving load analysis was performed to obtain maximum positive and negative moments.

The next step was to determine how much shallower could the superstructure depth be for the traditional systems if LLDFs for moment computed from FEA were used instead of those calculated based on AASHTO LFRD Specifications [8]. This information will be useful in determining how big of a benefit does a more accurate computation of live load distribution factors provide in terms of supplying a shallower superstructure depth. Once the shallowest superstructure depth for the traditional systems was obtained, the proposed systems were designed to maintain the same depth and a comparison in terms of weight and the number of strands required was performed.

The final exercise in terms of comparison was to determine whether the proposed systems could supply a shallower superstructure depth compared to the absolute minimum obtained for the traditional systems. The superstructure depth for the proposed systems was made 2 in. shallower than the absolute minimum for the traditional systems and the required number of strands was determined. It was outside the scope of work to determine the absolute minimum superstructure depth for a given span for the proposed systems because the main goal was to demonstrate that the proposed systems are competitive with the traditional systems.

Although it was expected that flexural tensile stresses at service would control the design, a shear check was performed to ensure that all investigated cases worked for shear using a practical arrangement of shear reinforcing.

Longitudinal Connections

The type of longitudinal connections between adjacent precast members plays an important role in emulating monolithic action. Figure 9 illustrates two types of connections that can be used along the longitudinal joints between adjacent precast members for the topped systems. The proposed connections can be used when the precast webs are tapered and straight. Both are discrete connections spaced at 4 ft on center. In the first connection a pocket is created in the bottom flange of the precast beam. The dimensions of this pocket are 6 in. in the transverse direction, 3 in. deep and 12 in. in the longitudinal direction. Two top bars from the bottom precast flange protrude through the pocket. After the adjacent precast beams are placed next to each other, site installed bars are placed to lap the protruding bars. The pocket is filled with ultra-high performance concrete to benefit from the shorter lap length supplied when such concrete is used. When concentrated loads, such as truck wheel loads, are applied the superstructure of the bridge bends in the transverse direction in addition to bending in the longitudinal direction due to plate action. This creates transverse bending moments. The purpose of the connections along the longitudinal joints is to resist these transverse bending moments by providing a tension tie at the bottom flange where tensions exist. The size of

the bars will depend on the actual tensile force applied to the connection due to the transverse bending moment.

The second connection is a welded connection and features discrete inclined embedded steel plates at 4 ft on center. The precast flanges are connected by field welding a smooth bar to each embedded steel plate using partial penetration welds. The embedded steel plate is inclined so that it can receive the smooth bar as well as accommodate any differences in elevation due to camber variations in precast beams. Top and bottom bars are welded to the back of the inclined steel plates using complete penetration welds. These bars can be either continuous or lapped with the bars coming from the opposite side at mid-width of the bottom flange to provide tolerance during construction. The projected depth of the embedded steel plate is 5.25 in. to allow for a $\frac{3}{4}$ chamfer at the bottom of the precast flange. The length of the embedded steel plate can be 12 in. to accommodate two bars welded to it spaced 6 in. apart. The thickness of the plate and the size of the bars will depend on the actual tensile force applied to the connection due to the transverse bending moment. A $\frac{3}{4}$ in thick plate is suggested as a starting point. After the site installed smooth bar is installed, the V-shaped space can be filled with non-shrink grout to provide protection to the smooth bar and embedded steel plates.

One of the advantages of PS3 compared to PS4 with respect to completing the longitudinal connections on site is the added space between the adjacent members because of the tapered webs. This additional space should help the contractor during the placement of the UHPC fill if the UHPC connection configuration is used, or during the field welding process if the welded connection option is used. However, the straight webs provided in PS4 shorten the span for the 2 in. SIP concrete forms and also for the composite deck when it is subject to wheel loads.

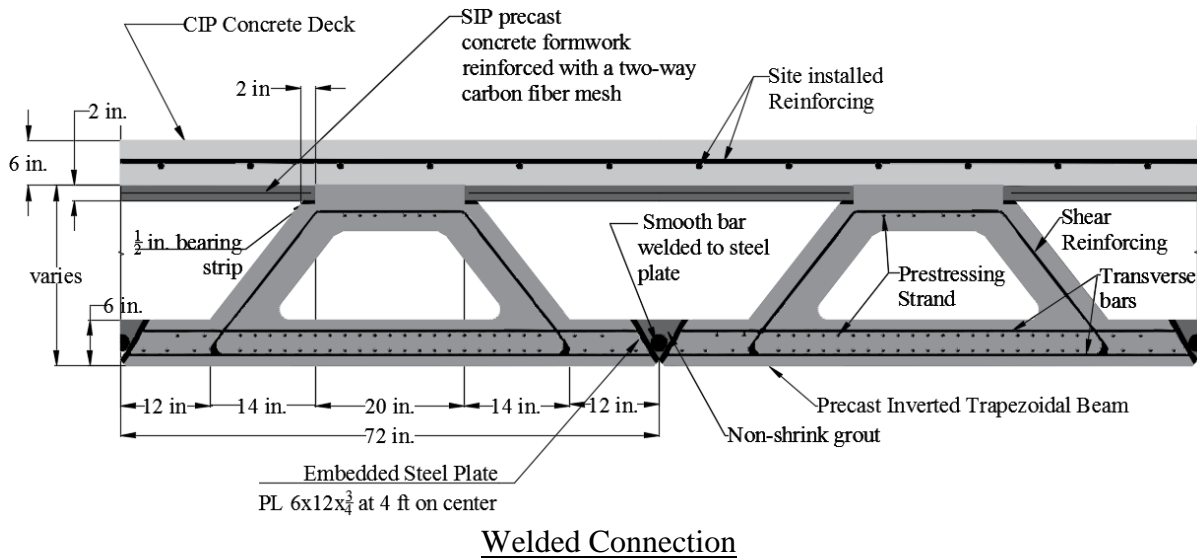
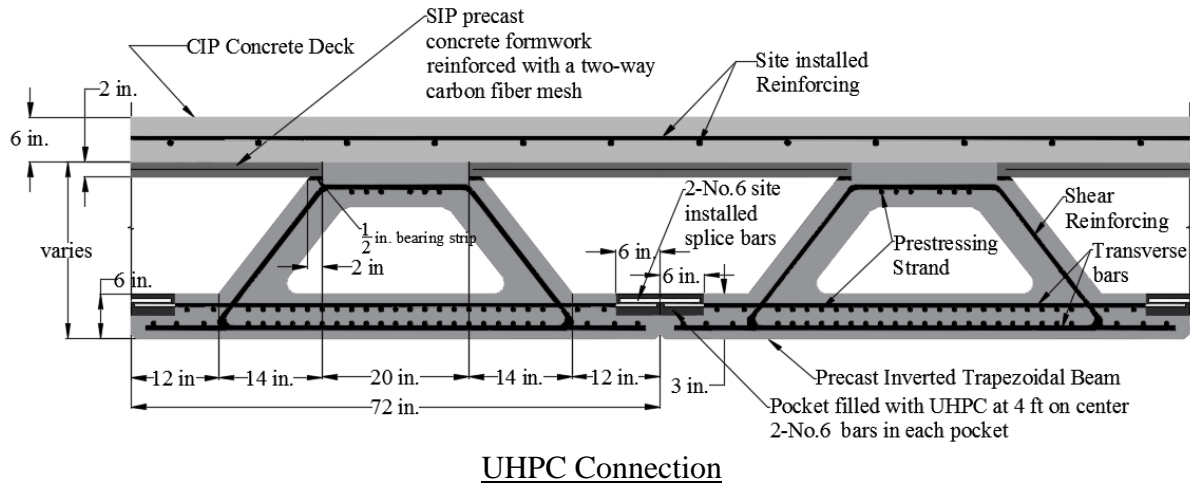


Figure 9
Longitudinal connections for topped systems

The tension force in the longitudinal connections was calculated by recording the transverse normal stress in the 3D solid elements in the bottom precast flange and by multiplying it with the area of the elements that were part of the transverse connection. The discrete connections in the bottom precast flange of the topped systems were modeled by using discrete tie constraints between the finite elements that fell within the region of the longitudinal connections (Figure 10). Two layers of finite elements were used in the bottom precast flange. The thickness of the flange is 6 in., so, the depth of each finite element in the bottom flange was 3 in. Given that a 3 in. mesh was used for the bottom precast flange, four of the finite elements in the top layer of the bottom flange were tied with those corresponding to the adjacent member. As a result, the area of the tie constraint between the adjacent members was 3 in. deep and 12 in. long. The spacing of the discrete ties was 4 ft to match the specified

spacing of the longitudinal connections.

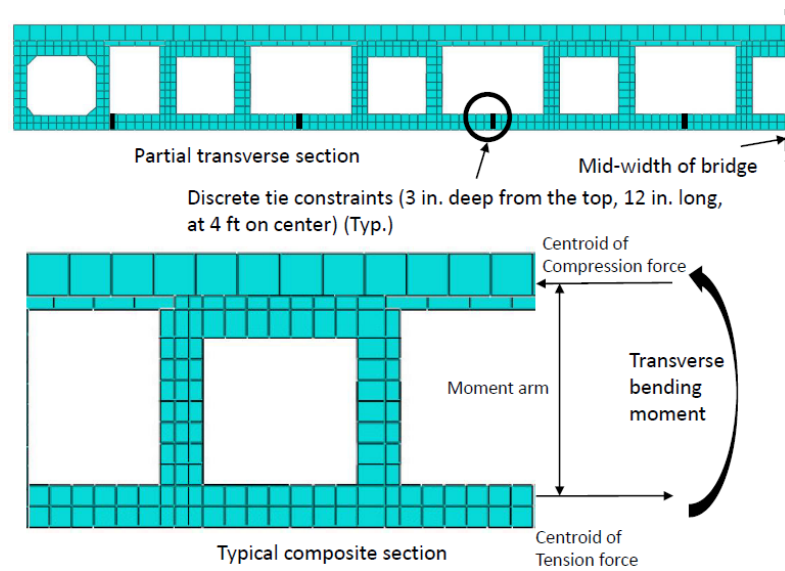


Figure 10
Calculation of transverse tensile force in proposed topped systems

Figure 11 illustrates the proposed connection along the longitudinal joints for the un-topped systems. This connection is based on the work performed by French et al. on decked bulb tees [7]. This is a continuous connection and features No.5 deformed wire reinforcing U-shaped bars. Stainless steel U-bars are also an alternative. The inside bent diameter for the No.5 U-shaped bars is $3d_b$ to ensure that the U-shaped bars fit in the 6 in. flange. This bend diameter is smaller than the $6d_b$ requirement in AASHTO for a No.5 bar made of conventional steel. It is also smaller than the $4d_b$ bent diameter required for D31 deformed wire reinforcement (DWR) when it is used as stirrups or ties. However, such a smaller bent diameter was considered acceptable because of the additional ductility of deformed wire reinforcing or stainless steel bars.

The U-bars are oriented vertically in the joint to provide two layers of reinforcement fabricated with a single rebar. The U-bars provide continuity for the precast flange reinforcing in the proposed systems across the joint by lapping with the U-bars from the adjacent flanges. The 180° bend of the U-bar, embedded in the joint, provides mechanical anchorage, which is necessary to minimize the required lap length (French et al. [7]). The U-bars are staggered with the adjacent U-bars to facilitate construction. However, the stagger should not be too large, otherwise the transfer of forces across the joint may be affected. To address this, a No.4 lacer bar is provided to help connect the U-shaped bars in the longitudinal direction. The inclusion of lacer bars was based on the work performed by

Gordon and May who conducted tests on loop bar joints with and without lacer bars and found that the presence of the lacer bars improved the performance of the test specimens [14]. A shear key is provided at the ends of the precast flanges. A closure pour provides continuity between the adjacent members. The width of the closure pour at the top and bottom of the precast flange is 8 in, and the width at mid-depth of the precast flange is 11 in. The lap length from the inside of U-bar to the inside of U-bar is 6 in. The cover to the top steel is 2 in. and the cover to the bottom steel is 7/8 in. The shear key surfaces should be cleaned to remove all contaminants that could interfere with adhesion. Additionally, the surfaces of the shear key should be sandblasted to prepare the joint for the closure pour. Sandblasting should help with developing a surface roughness that promotes good mechanical bond between the closure pour material and precast concrete. The study by French et al. included two types of closure pour materials. The first was a SET45 HW grout for overnight cure and the second was a high performance concrete (HPC) mix for 7 day cure [7]. The grout formulation was investigated both without extension and with 60% extension. The uniform-sized sound 0.25-0.5 in. round pea gravel used to extend the grout was tested with 10% HCL to confirm that it was not calcareous (French et al. [7]). Similar closure pour materials are proposed for the un-topped systems.

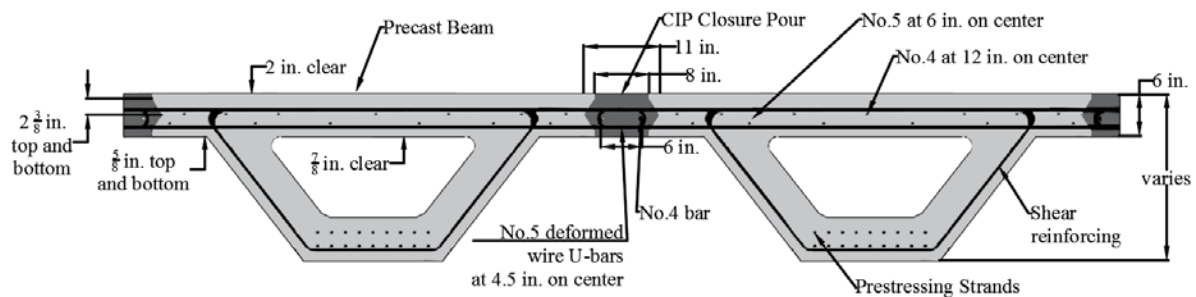


Figure 11
Longitudinal connection for un-topped system

The design compressive strength in the proposed un-topped systems is 8 ksi, which is larger than the 7 ksi design compressive strength used in deck panel testing by French et al. [7]. The nominal yield stress used for the deformed U-shaped bars by French et al., was 75 ksi [7]. During the material characterization study both deformed wire and stainless steel options were pursued, however during deck panel testing the deformed wire was used due to the reduced cost. The overall deck panel depth was 6.25 in., which is 1/4 in. greater than the proposed precast flange thickness in the un-topped systems.

Several finite element analyses were conducted with the purpose of determining the worst case transverse bending moment in the proposed un-topped bridge systems. The magnitude of the transverse bending moment will dictate the spacing of the U-shaped No.5 bars. Because of the tight clearances and reduced bar bend diameters it is recommended that the U-shaped bars are either No. 5 or smaller. Numerical simulations included at least two layers of finite elements in the top precast flange even though bending effects could be captured with one layer of 3D solid elements with incompatible modes (Figure 12). The transverse bending moment per one foot of length was calculated by recording the transverse compression and tensile forces in the top and bottom finite elements and multiplying them with the moment arm. In lieu of performing a plate analysis, AASHTO's strip method for deck design may be used to determine transverse bending moment demands. This is discussed further in the results section of this report.

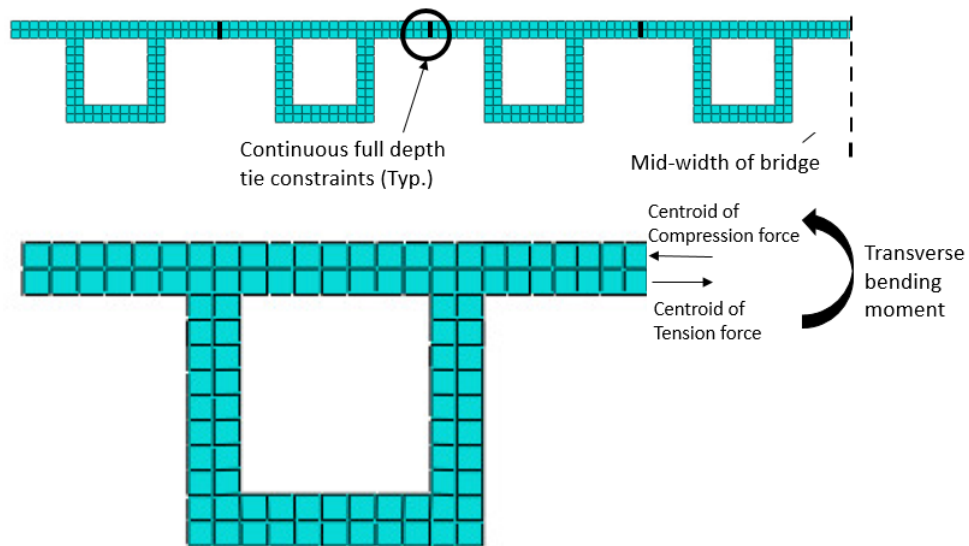


Figure 12
Calculation of transverse bending moment in un-topped systems

DISCUSSION OF RESULTS

Live Load Distribution Factors

To be able to perform a consistent comparison between the proposed systems and the traditional systems, live load distribution factors (LLDF) for moment for all systems were computed using finite element analyses. Figure 13 illustrates the LLDFs computed for each system. The LLDFs computed for PS1 and PS2 were compared with those computed for the adjacent box beam system and those calculated based on AASHTO provisions for adjacent box beam bridges. The traditional adjacent box beam system featured the lowest computed LLDFs compared to PS1 and PS2. AASHTO provisions led to LLDFs that were higher than those computed using finite element analysis. However, the computed LLDFs for moment for the proposed topped systems were similar to those calculated based on AASHTO provisions for the adjacent box beams system. As a result AASHTO provisions can be used to conservatively and reasonably calculate LLDFs for moment for the proposed topped systems.

PS3 and PS4 featured lower LLDFs compared to the traditional decked bulb tee system for all spans. Additionally, the computed LLDFs for moment for the proposed un-topped systems were significantly lower than those calculated based on AASHTO provisions for the traditional decked bulb tee system. The computed LLDFs for the decked bulb tee system were also lower than those calculated using AASHTO provisions. As a result, while AASHTO provisions may be used conservatively to calculate LLDFs for moment for the proposed un-topped systems, the designer may also use the values provided in this report if a more accurate estimation of LLDFs is desired. The use of more accurate LLDFs may play a determining role when choosing a superstructure depth for bridges built on sites with stringent vertical clearance requirements.

Figure 14 illustrates the LLDFs for shear for all investigated systems. Unlike LLDFs for moment the difference between computed LLDFs and those calculated based on AASHTO provisions is significant. The computed LLDFs for shear are less than half of those calculated based on AASHTO provisions. Therefore, if a more economical shear design is pursued, the computed LLDFs for shear presented in the report may be used in lieu of those calculated based on AASHTO provisions. There was not a significant difference between the computed LLDFs for shear in the proposed systems and traditional systems.

LLDFs for the normal weight and lightweight concrete options were similar. When lightweight concrete was used the beams deflected more compared to the normal weight option, however this resulted in similar LLDFs for moment. The difference in deflections and

camber between the normal weight and lightweight concrete options is discussed later in this report.

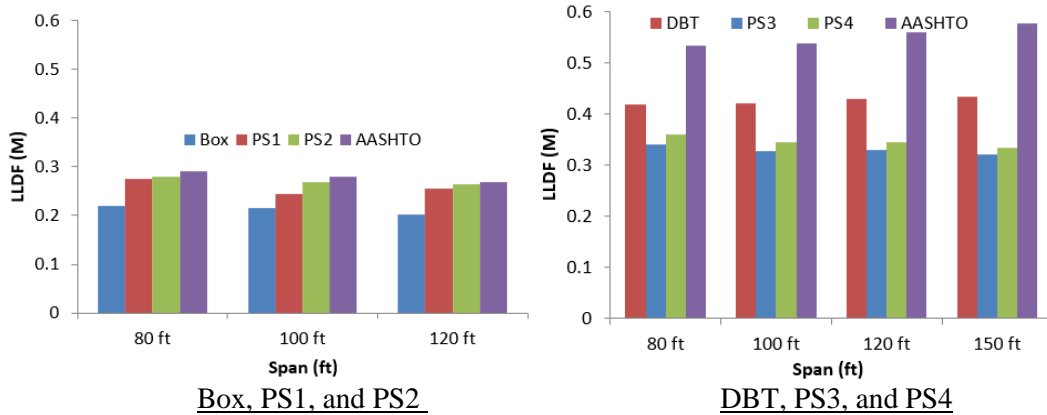


Figure 13
Comparison of LLDFs for moment

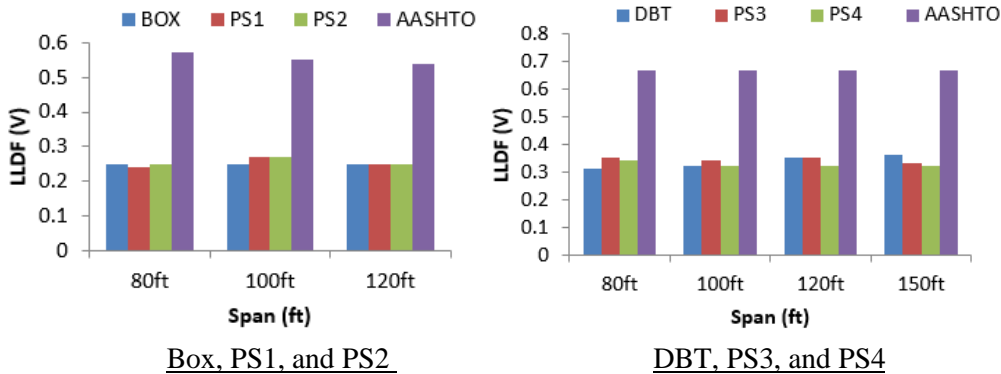


Figure 14
Comparison of LLDFs for shear

A variety of cases were considered when determining live load distribution factors. Superstructures with and without barriers were analyzed and it was found that when the barrier was omitted LLDFs for moment were higher. Additionally, the presence of a continuous structural barrier cannot always be relied upon. As a result, all reported LLDFs were obtained from models that featured no barrier. From the investigated load positions the ones that featured edge loading resulted in higher LLDFs. This is expected because when the truck or tandem is positioned along the edge of the superstructure there is limited opportunity to share the load with the adjacent members as opposed to the case when the load is applied at mid-width, and the adjacent members on both sides can be used to share the load. Figure 15 shows the LLDFs for moment for the 80 ft span for both topped and un-topped systems. The loading in this case is edge loading and the exterior girders are loaded the most. As noted

above the proposed topped systems featured higher LLDFs for moment compared to the traditional box system. Conversely, the proposed un-topped systems featured lower LLDFs for moment compared to the traditional decked bulb tee system.

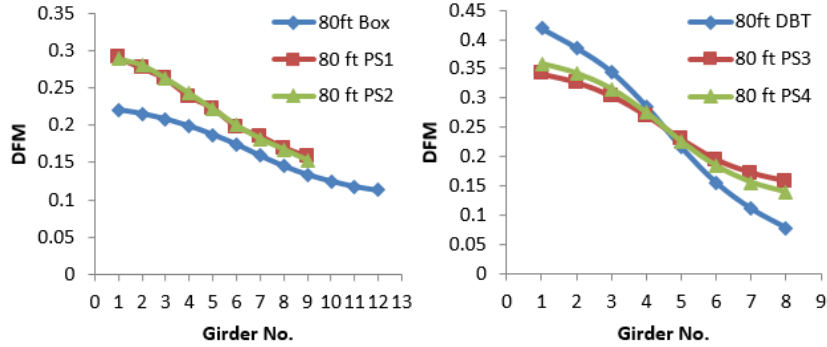


Figure 15
LLDF for moment in each beam for the 80 ft span

Load cases that featured truck plus lane and tandem plus lane loading were considered. It was determined that both cases resulted in similar LLDFs. The multiple presence effect was considered by loading multiple lanes and by multiplying the computed LLDFs by the multiple presence factors provided in AASHTO. It was determined that the case that featured a two truck loading configuration controlled over the other cases.

A mesh sensitivity analysis was performed to determine whether the computed LLDFs were influenced by the size of the finite elements. This exercise was done for the 80 ft span decked bulb tee system. Four different mesh sizes were considered, 3 in., 4.5 in., 6 in., and 7.5 in. Figure 16 illustrates the results of the mesh sensitivity analysis for the decked bulb tee system and demonstrates that the mesh size did not make a difference in terms of LLDFs.

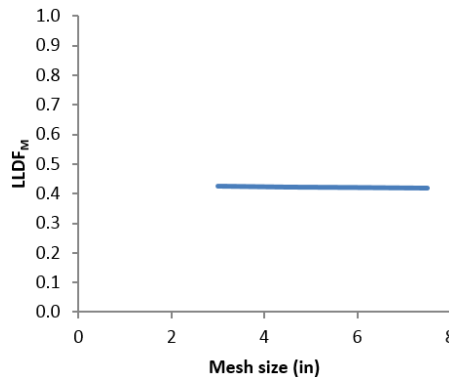


Figure 16
Mesh sensitivity analysis (LLDF_M for DBT 80 ft span)

Design of Superstructure Systems

Validation

All bridge systems were designed using AASHTO provisions using Mathcad [8], [9]. The results obtained from Mathcad in terms of number of strands for the traditional systems were compared with those obtained from the PCI Bridge Design Manual and Conspan (Table 2 and Table 3) [9], [12], [10]. During this comparison the LLDFs were based on AASHTO provisions [8]. The number of strands for a typical precast beam was either identical or almost identical. This suggests that the design calculations used in Mathcad lead to reliable results [9]. The case that featured a decked bulb tee system in a 100 ft span configuration could not be analyzed and designed in Conspan because BT-41 was not in the Conspan database [10].

Table 2
Comparison of number of strands using various design tools (Box beams -NW)

Adjacent Box Beams						
Span (ft)	Type	Depth (in)	Width (ft)	No. of strands (0.6 in. diameter)		
				PCI Design Manual	MathCAD File	Conspan Software
80	BII - 48	33	4	17	17	17
100	BIII - 48	39	4	23	23	23
120	BIV - 48	42	4	31	31	32

Table 3
Comparison of number of strands using various design tools (DBT - NW)

Decked Bulb Tee						
Span (ft)	Type	Depth (in.)	Width (ft)	PCI Design Manual	MathCAD File	Conspan Software
80	BT-35	35	6	22	22	22
100	BT-41	41	6	32	30	NC*
120	BT-53	53	6	30	32	32
150	BT-65	65	6	38	38	38

NC* = Not computed because BT-41 is not in Conspan database

Topped Systems

The strand layout for each investigated case for the topped systems is illustrated in Figure 17, Figure 18, and Figure 19. A minimum strand spacing of 2 in. center to center was used in all designs. Also, the distance from the bottom or top of the precast beams to the center of the nearest layer of strands was taken equal to 2.0 in. For those systems that featured straight webs a portion of the strands were harped to control stresses at the ends. When normal

weight concrete was used, the total number of strands was higher compared to the lightweight concrete option. Table 4 and Table 5 illustrate the controlling parameters for the normal weight and light weight concrete options, respectively. Always the design of the bridge superstructure systems was controlled by the allowable tensile stresses at service at mid-span at the bottom of the beam. However, stresses at transfer particularly at the ends of the beam at the bottom were close to the allowable stresses and the ratio between the actual stress and the allowable stress while being less than that at mid-span at service was also close to 1.0. Live load deflections in all cases were smaller than allowable deflections calculated based on AASHTO provisions. All cases were checked for shear to ensure that a shear design complied with AASHTO provisions using a practical arrangement of stirrups.

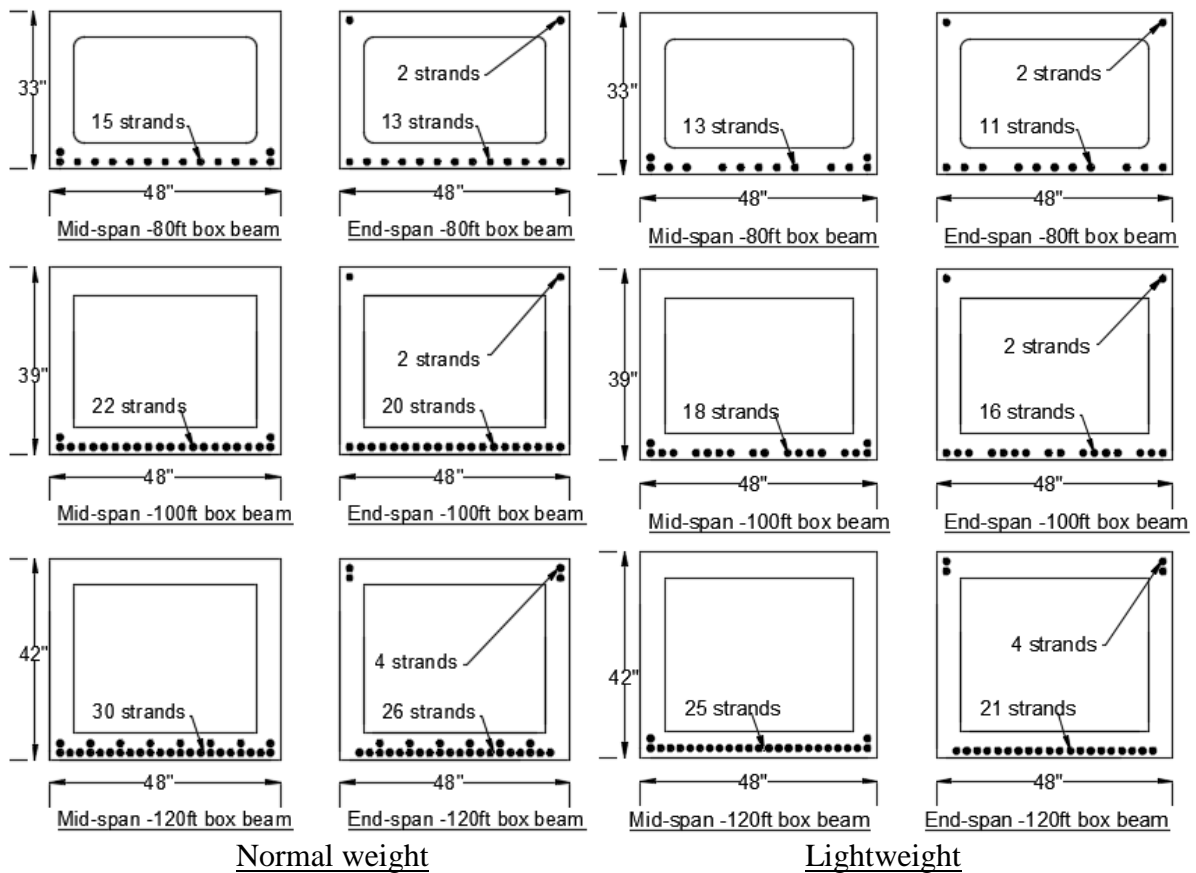


Figure 17
Strand configuration for Box beams

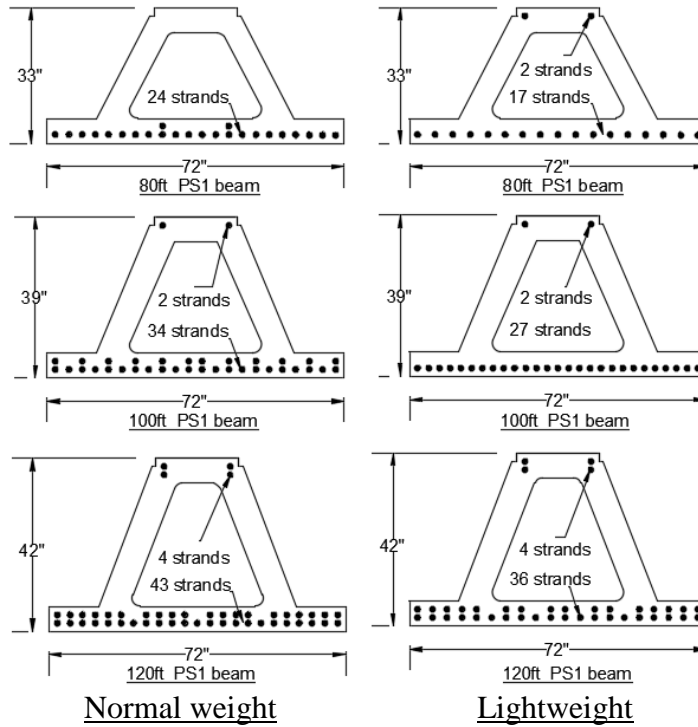


Figure 18
Strand Configuration for PS1

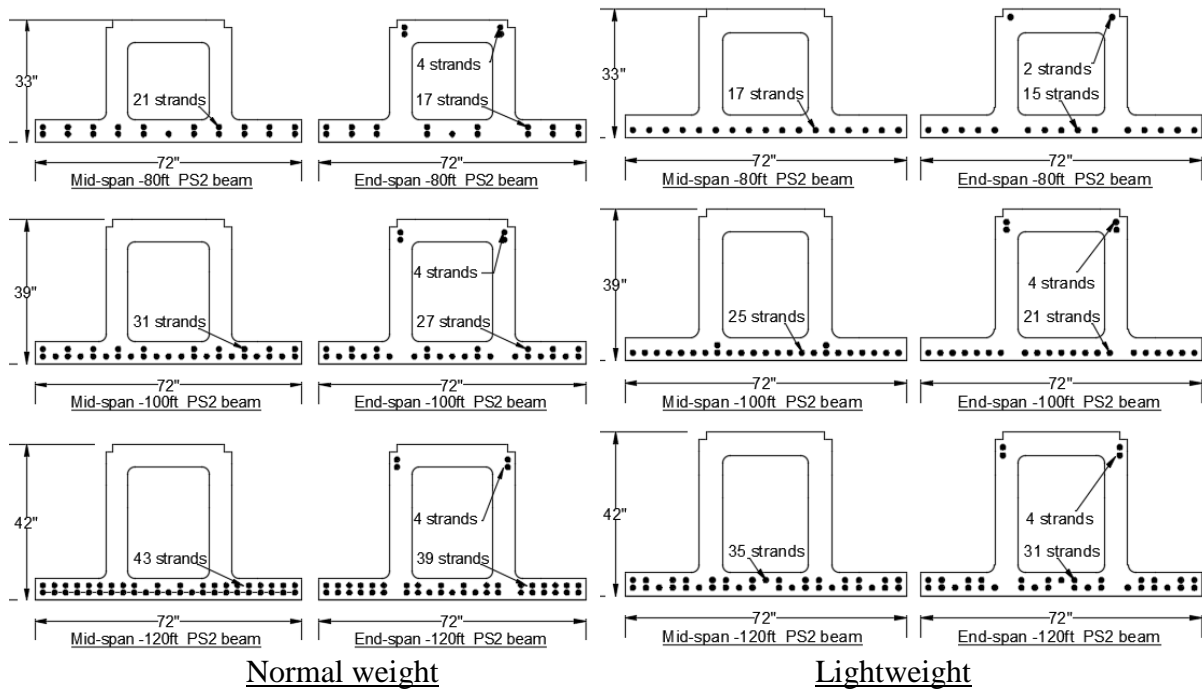


Figure 19
Strand configuration PS2

Table 4
Controlling parameters for the normal weight concrete option (topped systems)

Type	Span (ft)	Controlling Factor	Actual stress (ksi)	Allowable stress (ksi)	Ratio (Actual/Allowable)
Box	80	Service-Bottom of beam- Mid-span	0.518	0.537	0.96
	100	Service-Bottom of beam- Mid-span	0.514	0.537	0.96
	120	Service-Bottom of beam- Mid-span	0.523	0.537	0.97
PS1	80	Service-Bottom of beam- Mid-span	0.505	0.537	0.94
	100	Service-Bottom of beam- Mid-span	0.528	0.537	0.98
	120	Service-Bottom of beam- Mid-span	0.528	0.537	0.98
PS2	80	Service-Bottom of beam- Mid-span	0.526	0.537	0.98
	100	Service-Bottom of beam- Mid-span	0.507	0.537	0.94
	120	Service-Bottom of beam- Mid-span	0.529	0.537	0.99

Table 5
Controlling parameters for the lightweight concrete option (topped systems)

Type	Span (ft)	Controlling Factor	Actual stress (ksi)	Allowable stress (ksi)	Ratio (Actual/Allowable)
Box	80	Service- Bottom of beam- Mid-span	0.503	0.537	0.94
	100	Service- Bottom of beam- Mid-span	0.519	0.537	0.97
	120	Service- Bottom of beam- Mid-span	0.506	0.537	0.94
PS1	80	Service- Bottom of beam- Mid-span	0.533	0.537	0.99
	100	Service- Bottom of beam- Mid-span	0.511	0.537	0.95
	120	Service- Bottom of beam- Mid-span	0.528	0.537	0.98
PS2	80	Service- Bottom of beam- Mid-span	0.504	0.537	0.94
	100	Service- Bottom of beam- Mid-span	0.523	0.537	0.97
	120	Service- Bottom of beam- Mid-span	0.520	0.537	0.97

Deck Design

The SIP forms for the proposed topped systems were designed to support their self-weight, the weight of the wet concrete topping, and 20 psf construction loads without incurring any cracking at service. Table 6 provides a summary of the results of the design of the precast SIP forms for the aforementioned loads. The design was performed for a one foot strip. The cracking moment was larger than the moment created by the loads during the placement of the CIP topping. Therefore no cracking is expected to occur during this operation. The factored moment due to the loads during the placement of the CIP topping was also smaller than the flexural strength of the precast SIP forms.

Table 6
Design of precast concrete SIP forms

System	Material		Service			Ultimate	
	Concrete	C-grid	M _{service} (ft-kips)	M _{cr} (ft-kips)	Cracked?	M _u (ft-kips)	φM _n (ft-kips)
Tapered	f' _c = 4 ksi	One layer	0.26	0.32	No	0.35	0.50
Straight	f' _c = 4 ksi	One layer	0.17	0.32	No	0.22	0.50

The topping and the SIP forms were designed compositely to support any superimposed live loads without incurring any cracking at service. At the ultimate limit state the composite deck was designed by taking into account the presence of the C-grid and reinforcing steel when estimating the nominal flexural strength. AASHTO's strip method was used to design the composite deck. The maximum moment demand at service and at ultimate was determined by performing a moving load analysis for the superimposed design live loads. The cracking moment was calculated by using gross cross-sectional properties and by ignoring the presence of steel and C-grid. The cracking moments for the composite deck in both proposed systems were higher than positive and negative moments at service. The negative moment capacity for PS1 was 6% smaller than the negative factored moment at ultimate. However, given that the difference between the positive flexural moment capacity and the factored positive moment was 58%, moment redistribution can be used to address the difference between negative moment capacity and demand.

Table 7
Design of composite deck

System	Material				Service			Ultimate	
	SIP		Topping		M _{service} (ft-kips)	M _{cr} (ft-kips)	Cracked ?	M _u (ft-kip)	φM _n (ft-kip)
	Concrete (ksi)	C grid	Concrete (ksi)	Steel (ksi)					
Tapered	f' _c =4	One layer	f' _c =4	f _y =60	+13.5	+28.0	No	+23.4	+37.0
					-13.6	-28.0	No	-23.4*	-22.0*
Straight	f' _c =4	One Layer	f' _c =4	f _y =60	+12.0	+28.0	No	+21.0	+37.0
					-10.5	-28.0	No	-18.0	-22.0

*Considered acceptable because of moment redistribution

Material Use

The use of material for the topped systems was compared in terms of composite and non-composite weights, as well as number of strands. Figure 20 provides the comparison in terms

of composite and non-composite weights for all topped systems. The width of adjacent precast box beams is 4ft, whereas the width of the proposed precast beams is 6 ft. Therefore the weight of the traditional box beam system is for a 6 ft transverse width to make a consistent comparison. The traditional box system is the heaviest. PS1 is the lightest system and PS2 is ranked second. As a result, in terms of weight both proposed systems offer a lighter superstructure for both normal weight and lightweight concrete options compared to the traditional adjacent box beam system. A lighter superstructure is desired in terms of reducing the load demand on the substructure components. Additionally, for those bridges constructed in seismic regions, a lower superstructure weight helps reduce the seismic load demand on the lateral load resisting system.

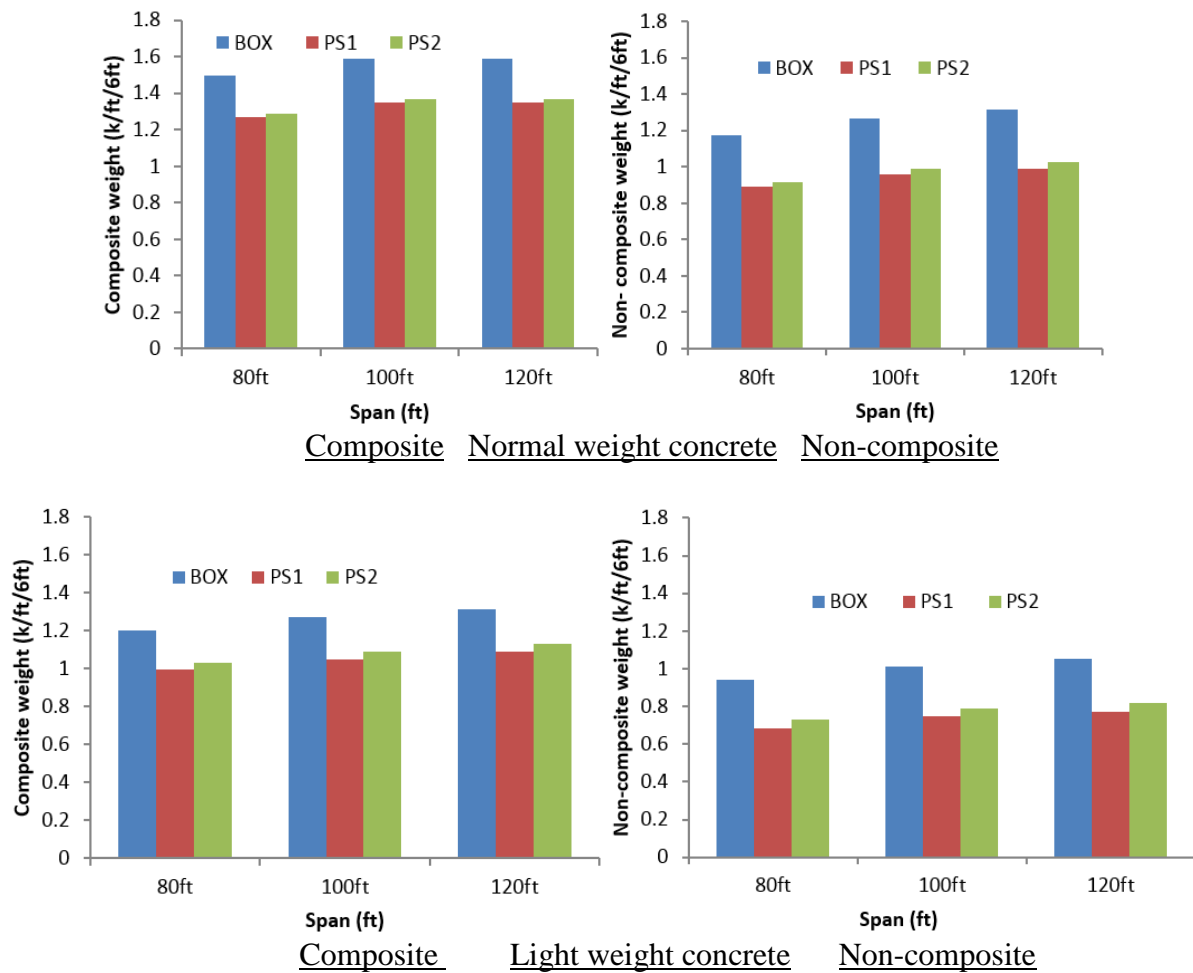


Figure 20
Composite and non-composite weights of individual precast beams (topped systems)

Figure 21 illustrates the total number of strands used in each topped system. The number of strands for the traditional box beam system is for a 6 ft transverse width to make a consistent

comparison with the proposed systems. PS2 requires the lowest number of strands. PS1 is ranked second. Tables 6 and 7 provide a summary of the information provided in Figure 20 and Figure 21 as well as the ratio between the weight and number of strands of the proposed systems over the traditional box beam system. The weight ratio is always smaller than one which suggests a more economical use of concrete and a lighter superstructure. The strand ratio for PS2 is also smaller than one, which suggests a more economical use of strands. For PS1 the strand ratio is slightly over one and the weight ratio is smaller than one which suggest a competitive use of materials compared to the traditional box system.

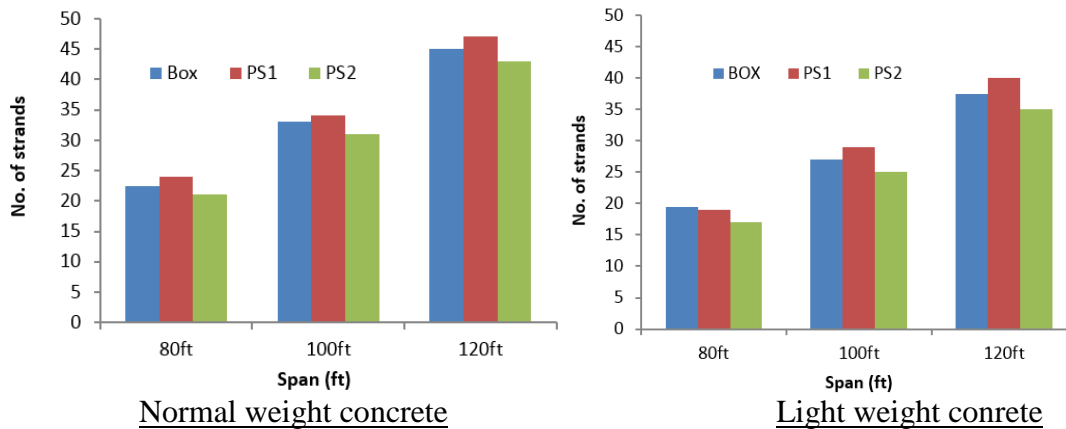


Figure 21
Number of strands per 6 ft of width (topped systems)

Table 8
Materials use comparison (normal weight)

Span (ft)	Type	Span to depth ratio	Concrete material (kip/ft/6ft)*				No. of strands**	
			Composite		Non composite		No.	Ratio (PS/Box)
			Weight	Ratio (PS/Box)	Weight	Ratio (PS/Box)		
80	Box	29.1	1.50	1.00	1.18	1.00	23	1.00
	PS1	29.1	1.27	0.85	0.89	0.76	24	1.04
	PS2	29.1	1.29	0.86	0.92	0.78	21	0.91
100	Box	30.8	1.59	1.00	1.27	1.00	33	1.00
	PS1	30.8	1.35	0.85	0.96	0.75	34	1.03
	PS2	30.8	1.37	0.86	0.99	0.78	31	0.94
120	Box	34.3	1.63	1.00	1.32	1.00	45	1.00
	PS1	34.3	1.39	0.85	0.99	0.75	47	1.04
	PS2	34.3	1.41	0.86	1.03	0.78	43	0.96

*The weight for the box beam system is for 6 ft of transverse width, The weight for the proposed topped systems is for a single precast beam, which is 6 ft wide, **Number of strands for box beams is for 6 ft of transverse width, No. of strands for PS systems is for a single precast beam, which is 6 ft wide.

Table 9
Materials use comparison (light weight)

Span (ft)	Type	Span to depth ratio	Concrete material (kip/ft/6ft)*				**No. of strands	
			Composite		Non composite		No.	Ratio (PS/Box)
			Weight	Ratio (PS/ Box)	Weight	Ratio (PS/ Box)		
80	Box	29.1	1.20	1.00	0.94	1.00	20	1.00
	PS1	29.1	0.99	0.83	0.68	0.73	19	0.95
	PS2	29.1	1.03	0.86	0.73	0.78	17	0.85
100	Box	30.8	1.27	1.00	1.01	1.00	27	1.00
	PS1	30.8	1.05	0.83	0.75	0.74	29	1.07
	PS2	30.8	1.09	0.86	0.79	0.78	25	0.93
120	Box	34.3	1.31	1.00	1.05	1.00	38	1.00
	PS1	34.3	1.09	0.83	0.77	0.73	40	1.05
	PS2	34.3	1.13	0.86	0.82	0.78	35	0.92

*The weight for the box beam system is for 6 ft of transverse width, The weight for the proposed topped systems is for a single precast beam, which is 6 ft wide, **Number of strands for box beams is for 6 ft of transverse width, No. of strands for PS systems is for a single precast beam, which is 6 ft wide.

Live load deflection and camber

Figure 22 illustrates the live load deflection and camber for all topped systems. The traditional adjacent box beam system features the lowest live load deflection. PS2 is ranked second in terms of live load deflection and PS1 is ranked 3rd. However, in all cases the live load deflection is smaller than the allowable deflection specified in AASHTO, which indicates that live load deflection is not a controlling parameter. With respect to camber the proposed systems typically feature lower cambers than the traditional adjacent box beam system. The only exception is the bridge with a 120 ft span and normal weight concrete. In this case the camber in PS2 is slightly larger than that in the box beam system. However, PS1 features the lowest camber in this case. Low cambers are desired because the lower the camber the lower the magnitude of positive restraint moments that will develop in the long term due to creep of concrete for bridges made continuous for live loads. Excessive positive restraint moments may cause cracking in the continuity diaphragm and affect the assumption about live load continuity. Also, one of the reasons why camber in the proposed systems is lower than that in the box beam system is the reduced eccentricity between the centroid of strands and the centroid of the precast beam. The bottom precast flange shifts the eccentricity of the precast section towards the bottom where almost all the strands are congregated. In the case of the adjacent box beams the eccentricity is larger thus resulting in a larger camber.

When lightweight concrete was used live load deflections and camber were higher compared to the normal weight concrete option. Because the overall depth of the superstructure was kept the same for all investigated systems for a given span, the reduction in material stiffness provided by lightweight concrete resulted in higher live load deflections and camber. Table 10 provides a summary of live load deflection and camber values and suggest that the proposed systems are stiffer than the traditional adjacent box beam system in terms of camber on an individual beam basis. However, the traditional box beam system features lower live load deflections on the completed composite bridge. This is attributed to the fact that the number of box beams in the completed bridge is larger than that for the proposed systems because the width of an individual box beam is 4 ft whereas the width an individual precast beam in PS1 and PS2 is 6 ft.

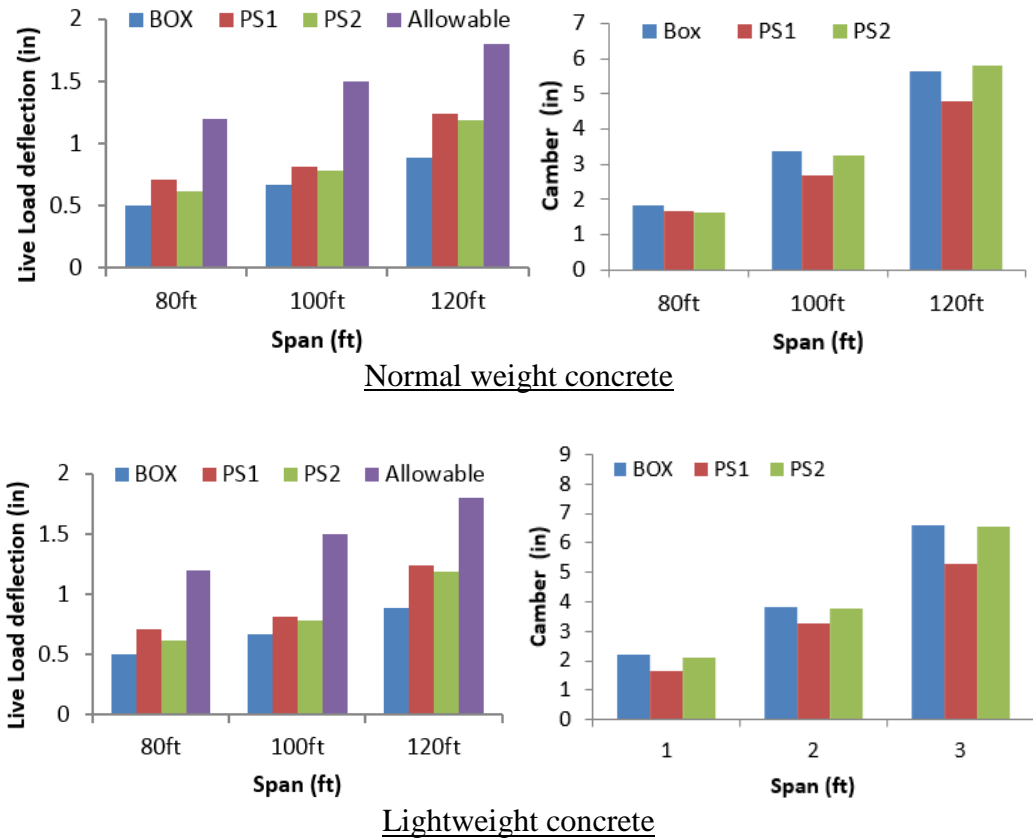


Figure 22
Live load deflection and camber comparison (topped systems)

Table 10
Summary of live load deflection and camber values

Parameter	Span (ft)	NW				LW			
		Box (in.)	PS1 (in.)	PS2 (in.)	Smallest	Box (in.)	PS1 (in.)	PS2 (in.)	Smallest
Live load Deflection	80	0.50	0.71	0.62	Box	0.70	0.99	0.87	Box
	100	0.66	0.81	0.78	Box	0.93	1.01	1.09	Box
	120	0.89	1.24	1.19	Box	1.25	1.74	1.66	Box
Camber	80	1.85	1.66	1.62	PS2	2.20	1.94	2.13	PS1
	100	3.36	2.69	3.24	PS1	3.80	3.26	3.76	PS1
	120	5.65	4.79	5.79	PS1	6.61	5.27	6.53	PS1

Shallower depths

The next step was to determine how much shallower could the superstructure depth be for the traditional system if LLDFs for moment computed from FEA were used instead of those calculated based on AASHTO LFRD Specifications. Table 11 provides superstructure depths for the box beam system for various spans. The typical superstructure depth was obtained from the PCI Bridge Design Manual and the shallowest superstructure depth was determined by designing the superstructure according to AASHTO LRFD Specifications using computed LLDFs for moment [12], [8]. The results in Table 11 suggest that the utilization of lower LLDFs computed from finite element analyses results in shallower superstructure depths for the traditional box system. The difference in heights varies from 4 in. to 6 in. The use of lightweight concrete results in slightly shallower superstructure depth but in general the shallowest superstructure depths for normal weight and lightweight concrete option for the box beam system are similar. Accordingly, when the depth of the superstructure is of concern, a more refined analysis in terms of LLDFs can result in a shallower superstructure and can help the designer meet the vertical clearance requirements present at the site.

Table 11
Superstructure depths for Box system

Superstructure System	Span (ft)	Typical height* (in.)	Shallowest height** NW (in.)	Shallowest height** LW (in.)
Box	80	33	29	28
	100	39	34	34
	120	42	38	37

*Obtained from PCI Bridge Design Manual [12], **Designed based on computed LLDFs

Once the shallowest superstructure depth for the traditional box system was obtained, the proposed systems were designed to maintain the same depth and a comparison in terms of the number of strands required was performed. Because PS2 was more competitive than PS1 with the box system, the number of strands required for the reduced superstructure depth was calculated only for PS2. Table 12 shows the composite weight for a transverse distance of 6 ft, and the number of strands required for the box system and PS2 systems when the reduced depth is used. Because the width of the precast box beams is 4 ft and the width of PS2 precast beams is 6 ft, the composite weight for a typical composite section was calculated for a distance of 6 ft to make a consistent comparison. PS2 continues to feature a smaller composite weight compared to the box beam system even for the shallowest box beam depth. This observation applies to both the normal weight and lightweight concrete options. Additionally, the number of strands required for the PS2 systems is less than that required for the box beam system. This continues to demonstrate the competitive use of the PS2 system.

Table 12
Weight and number of strands for PS2 and shallowest Box

Span (ft)	NW					LW				
	Height (in.)	Composite Weight (k/ft)*		No. of strands		Height (in.)	Composite Weight (k/ft)*		No. of strands	
		Box	PS2	Box	PS2		Box	PS2	Box	PS2
80	29	1.43	1.24	27	22	28	1.13	0.98	23	21
100	34	1.50	1.31	38	36	34	1.20	1.05	32	30
120	38	1.56	1.36	50	45	37	1.25	1.08	44	40

*Composite weight is for 6 ft of transverse width

The final exercise in terms of comparison was to determine whether the proposed systems could supply a shallower superstructure depth compared to the absolute minimum obtained for the traditional systems. The superstructure depth for the proposed systems was made 2 in. shallower than the absolute minimum for the traditional systems and the required number of strands was determined. It was outside the scope of work to determine the absolute minimum superstructure depth for a given span for the proposed systems because the main goal was to demonstrate that the proposed systems are competitive with the traditional systems.

Table 13 suggests that PS2 requires either a smaller or equal number of strands compared to the shallowest box beams system even though the superstructure depth is 2 in. shallower. Also, the composite weight continues to be smaller than the weight of the shallowest box beam system.

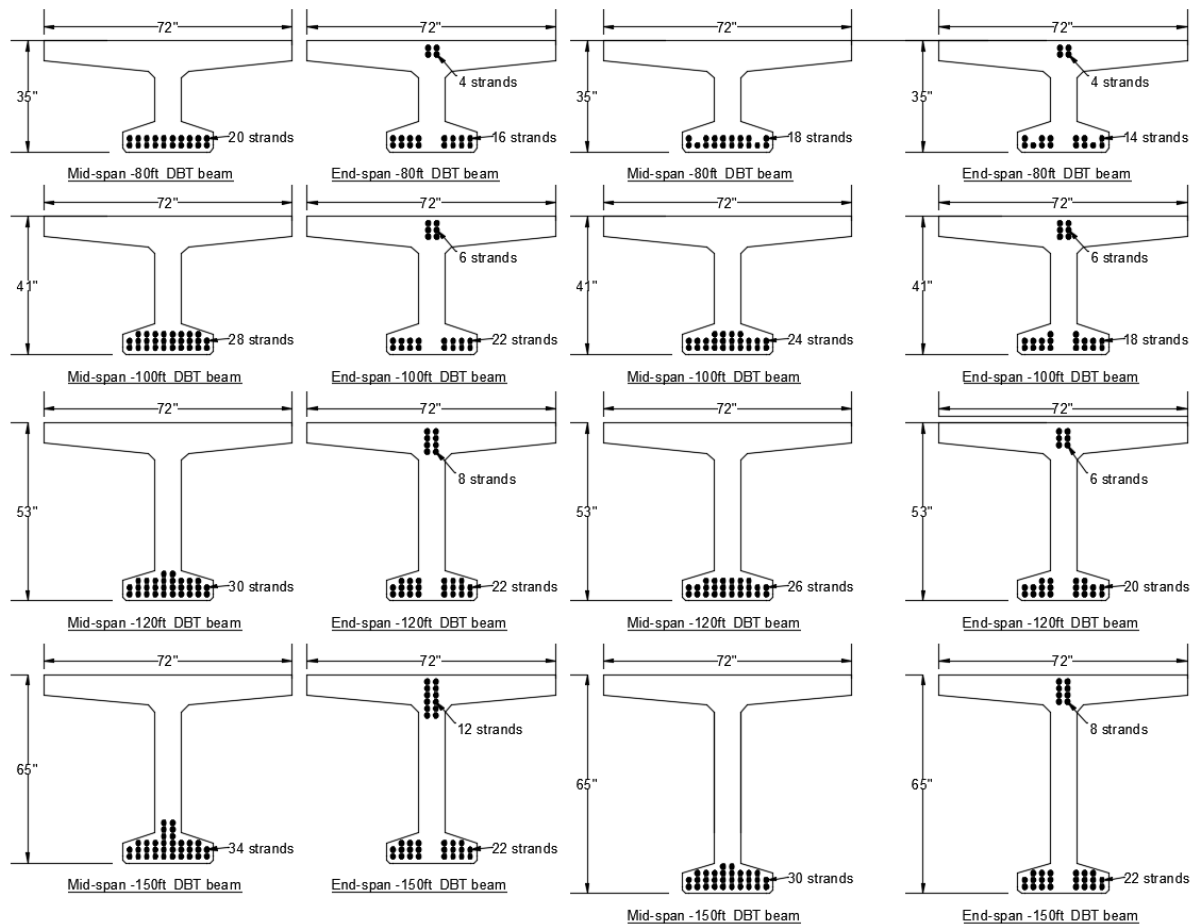
Table 13
Number of strands required for PS2 system for shallower superstructure depths

Span (ft)	NW			LW		
	Height (in.)	Composite Weight (k/ft)*	No. of strands PS2	Height (in.)	Composite Weight (k/ft)*	No. of strands PS2
80	27	1.22	26	26	0.97	22
100	32	1.28	38	32	1.02	32
120	36	1.33	50	35	1.06	42

*Composite weight is for 6 ft of transverse width

Un-topped Systems

The strand layout for each investigated case for the topped systems is illustrated in Figure 23, 24, and 25. A minimum strand spacing of 2 in. center to center was used in all designs. Also, the distance from the bottom or top of the precast beams to the center of the nearest layer of strands was taken equal to 2.0 in. For those systems that featured straight webs a portion of the strands were harped to control stresses at the ends. When normal weight concrete was used, the total number of strands was higher compared to the lightweight concrete option. One of the disadvantages of PS3 is the limited space to accommodate strands in the bottom flange. The width of the bottom flange in PS3 is 20 in., which is smaller than the width of the bottom flange in the traditional decked bulb tee system, which is 27 in. Because of the limited space to install strands in the bottom flange of the PS3 system, and the inability to harp strands because of the tapered webs, the strand layout sometimes had to extend in to the precast webs. Table 14 and 15 illustrate the controlling parameters for the normal weight and light weight concrete options, respectively. Almost always the design of the bridge superstructure systems was controlled by the allowable tensile stresses at service at mid-span at the bottom of the beam. Only in one case was the design controlled by the allowable compressive stress at transfer at the ends of the beam at the bottom. However, stresses at transfer particularly at the ends of the beam at the bottom were close to the allowable stresses and the ratio between the actual stress and the allowable stress while being less than that at mid-span at service was also close to 1.0. Live load deflections in all cases were smaller than allowable deflections calculated based on AASHTO provisions. All cases were checked for shear to ensure that a shear design complied with AASHTO provisions using a practical arrangement of stirrups.



Normal weight

Lightweight

Figure 23
Strand Configuration for Decked Bulb Tees

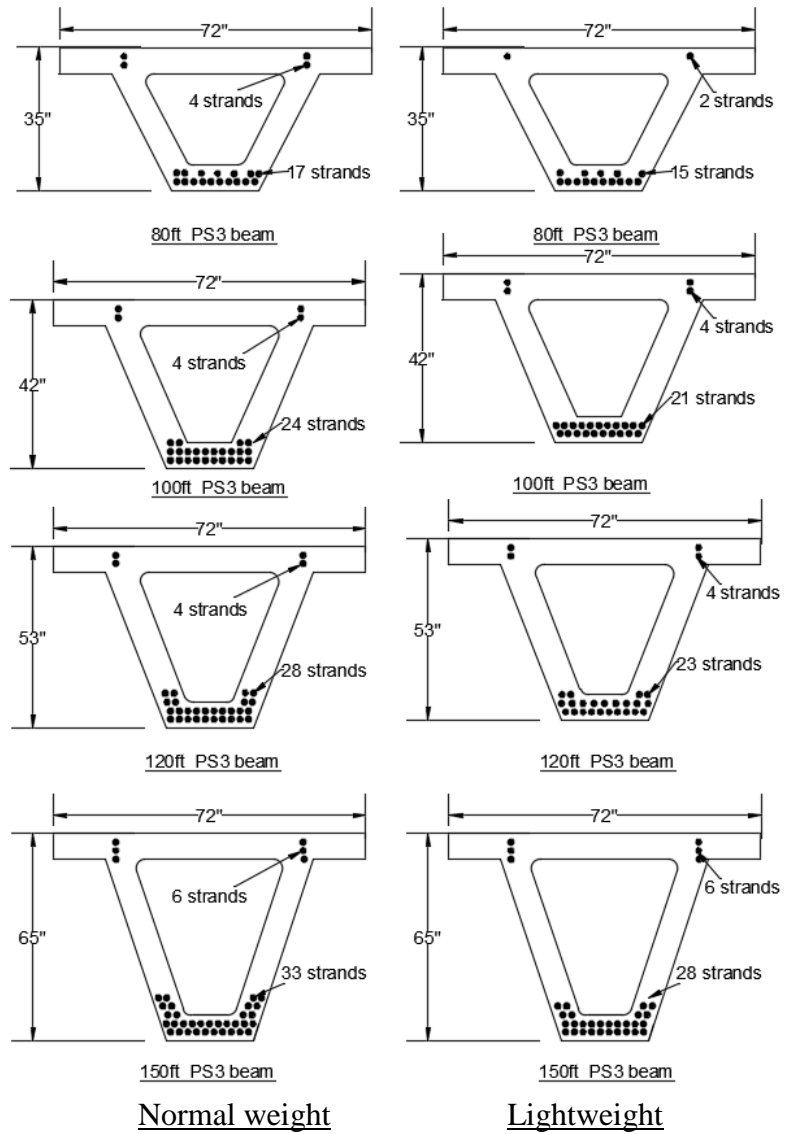


Figure 24
Strand configuration for PS3

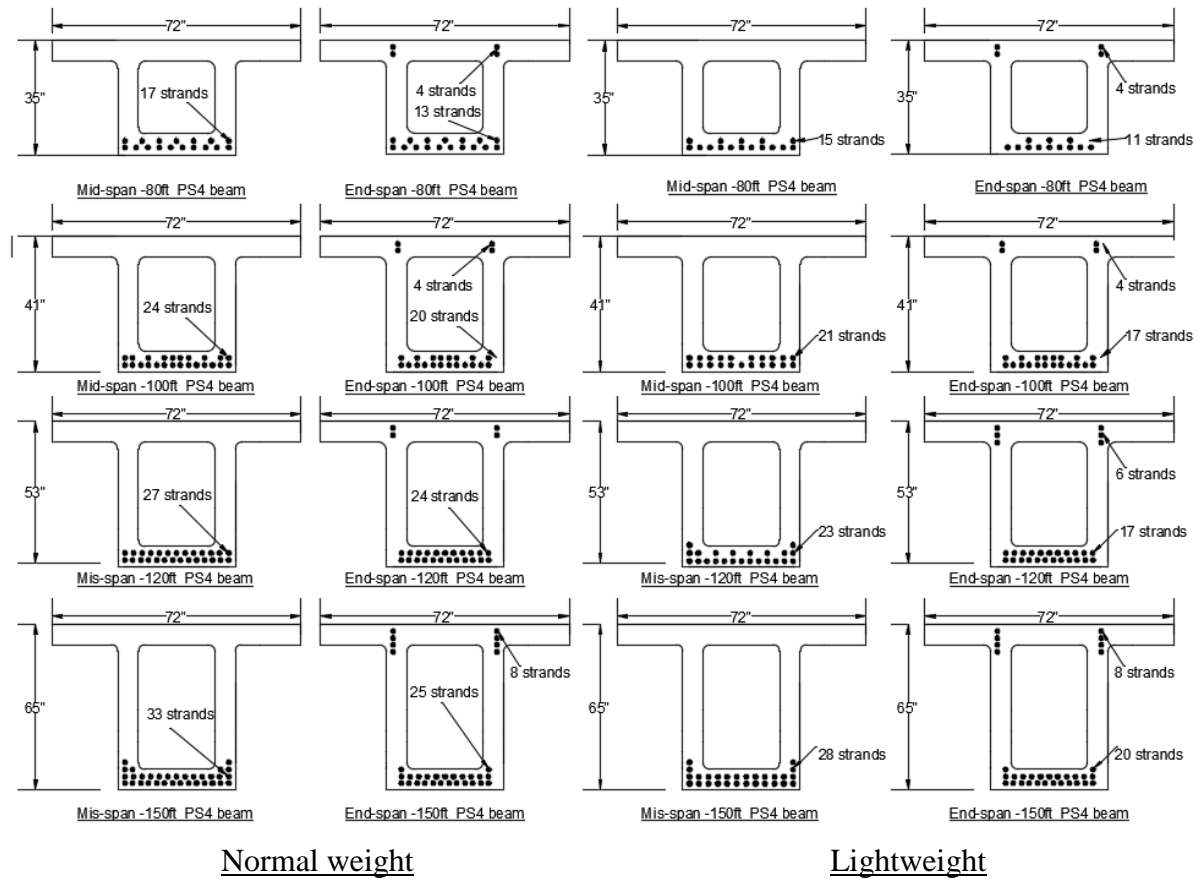


Figure 25
Strand configuration for PS4

Table 14
Controlling parameters (normal weight concrete) (un-topped systems)

Type	Span (ft)	Controlling Factor	Actual stress (ksi)	Allowable stress (ksi)	Ratio (Actual/Allowable)
DBT	80	Service-Bottom of beam- Mid-span	0.524	0.537	0.98
	100	Service-Bottom of beam- Mid-span	0.532	0.537	0.99
	120	Service-Bottom of beam- Mid-span	0.514	0.537	0.96
	150	Service-Bottom of beam- Mid-span	0.523	0.537	0.97
PS3	80	Service-Bottom of beam- Mid-span	0.518	0.537	0.96
	100	Service-Bottom of beam- Mid-span	0.505	0.537	0.94
	120	Transfer-Bottom of beam-End span	3.992	4.080	0.98
	150	Service-Bottom of beam- Mid-span	0.519	0.537	0.97
PS4	80	Service-Bottom of beam- Mid-span	0.517	0.537	0.96
	100	Service-Bottom of beam- Mid-span	0.510	0.537	0.95
	120	Service-Bottom of beam- Mid-span	0.501	0.537	0.93
	150	Service-Bottom of beam- Mid-span	0.519	0.537	0.97

Table 15
Controlling parameters (lightweight concrete) (un-topped systems)

Type	Span (ft)	Controlling Factor	Actual stress (ksi)	Allowable stress (ksi)	Ratio (Actual/Allowable)
DBT	80	Service- Bottom of beam- Mid-span	0.525	0.537	0.98
	100	Service- Bottom of beam- Mid-span	0.508	0.537	0.95
	120	Service- Bottom of beam- Mid-span	0.505	0.537	0.94
	150	Service- Bottom of beam- Mid-span	0.523	0.537	0.97
PS3	80	Service- Bottom of beam- Mid-span	0.511	0.537	0.95
	100	Service- Bottom of beam- Mid-span	0.528	0.537	0.98
	120	Service- Bottom of beam- Mid-span	0.518	0.537	0.96
	150	Service- Bottom of beam- Mid-span	0.534	0.537	0.99
PS4	80	Service-Bottom of beam - Mid-span	0.504	0.537	0.94
	100	Service-Bottom of beam - Mid-span	0.501	0.537	0.93
	120	Service-Bottom of beam - Mid-span	0.515	0.537	0.96
	150	Service-Bottom of beam - Mid-span	0.507	0.537	0.94

Top flange design

The top flange of the un-topped systems was designed for live loads in the transverse direction using AASHTO's strip method. A moving load analysis was performed to obtain maximum positive and negative moments in the transverse direction in the top precast flange. Table 16 provides a summary of the design of the top precast flange. Two sets of values are provided for maximum positive and negative moments at service and at ultimate. The values with no parentheses were calculated considering the presence of a barrier and the maximum moments in the top precast flange were recorded at the exterior precast beam. The values inside parentheses were computed for the case that featured no barrier. The presence of the barrier causes the maximum negative moment at service in the top precast flange of the exterior beam in the transverse direction to be greater than the cracking moment. Negative moments in the rest of the precast beams were smaller than the cracking moment. All positive moments were smaller than the cracking moment. The cracking moment was calculated using gross cross-sectional properties ignoring the presence of steel. When the barrier was removed, both negative and positive moments at service were smaller than the cracking moment. As a result, if no cracking is desired at service, the thickness of the precast flange of the exterior beam will need to be thicker than 6 in. Additionally, the top precast flange of the exterior beam will need to be designed to resist impact loads and a thicker precast flange may be warranted regardless of whether cracking is allowed or not at service. The flexural strength of the top precast flange in the transverse direction was calculated assuming transverse top and bottom reinforcing of No.5 deformed wire at 4.5 in. on center and was well above the computed maximum factored positive and negative moments. The

size and spacing of the bars in the transverse direction was dictated by the longitudinal connection between adjacent precast beams. This is discussed in detail under the section titled longitudinal connections.

Table 16
Top flange design for un-topped systems

System	Material		Service			Ultimate	
	Concrete f'_c (ksi)	Steel (ksi)	M_s^* (ft-kips)	M_{cr} (ft-kips)	Cracked?	M_u^* (ft-kips)	ϕM_n (ft-kips)
PS3	8	75	+16.5 +(17.1)	+/-22.1	No	+29.1 +(29.9)	+113
			-22.7 -(11.0)	+/-22.1	No*	-39.0 -(19.2)	-94
PS4	8	75	+14.5 +(13)	+/-22.1	No	+25.3 +(22.8)	+113
			-35.8 -(7.8)	+/-22.1	No*	-61.6 -(13.6)	-94

*The numbers with no parentheses are calculated assuming a barrier is present. The numbers in parentheses are calculated assuming that no barrier is present.

Material Use

The use of materials for the un-topped systems was compared in terms of the weight of the precast components, and number of strands required for a typical precast beam. Both normal weight and lightweight concrete options were investigated. Figure 26 illustrates the weight of the precast beams for all spans considered. The traditional decked bulb tee system is generally the lightest, which indicates its economy and efficiency. PS3 is ranked second in terms of weight because of the tapered webs, and PS4 is ranked 4th. In terms of the number of strands required, PS4 requires the least number of strands, however this comes at the expense of using more concrete than the traditional decked bulb tee system (Figure 27). PS3 required the largest number of strands because of the limited amount of space in the bottom precast flange and the inability to harp strands to control end stresses. Table 17 and Table 18 summarize the information provided in Figure 26 and Figure 27 and provide the ratios of weight and number of strands of the proposed systems over the traditional decked bulb tee system. The weight of the precast beams in the proposed system is no more than 19% of the traditional decked bulb tee system and in the case of PS4 the required number of strands is less than that required for the traditional system. This suggests that the proposed un-topped systems can be used competitively with the traditional decked bulb tee system. One of the advantages of PS4 is that it provides a more stable working platform for the installation of the closure pour and barriers compared to the decked bulb tee system because of the larger base at the bottom. The width of the bottom flange in the decked bulb tee system is 2 ft 3 in.

as opposed to 2 ft 10 in. in PS4.

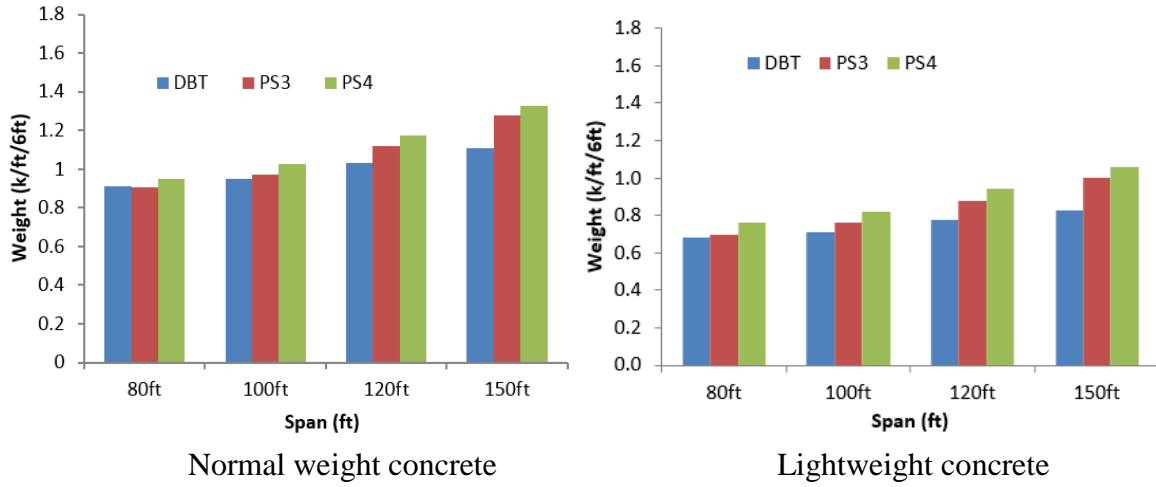


Figure 26
Material comparison between PS3, PS4 and DBT

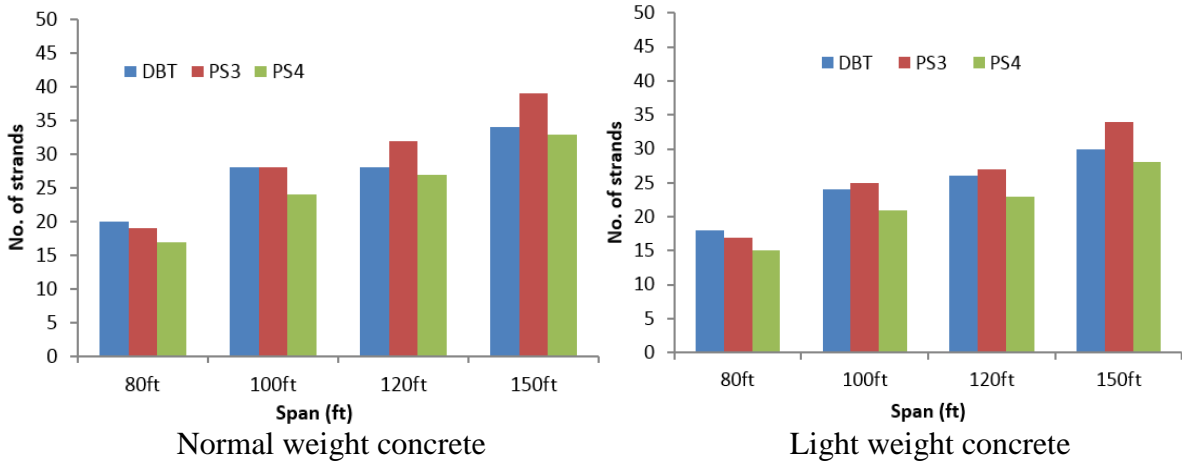


Figure 27
Number of strands comparison

Table 17
Materials use comparison (normal weight)

Span (ft)	Type	Span to depth ratio	Concrete material (kip/ft/6ft)		No. of strands	
			Composite = Non Composite		No.	Ratio (PS/DBT)
			Weight (kips)	Ratio (PS/ DBT)		
80	DBT	27.43	0.91	1.00	20	1.00
	PS3	27.43	0.90	0.99	19	0.95
	PS4	27.43	0.95	1.04	17	0.85
100	DBT	28.57	0.95	1.00	28	1.00
	PS3	28.57	0.97	1.02	28	1.00
	PS4	28.57	1.03	1.08	24	0.86
120	DBT	27.17	1.03	1.00	28	1.00
	PS3	27.17	1.12	1.09	32	1.14
	PS4	27.17	1.18	1.14	27	0.95
150	DBT	27.69	1.11	1.00	34	1.00
	PS3	27.69	1.28	1.15	39	1.15
	PS4	27.69	1.33	1.19	33	0.97

Table 18
Materials use comparison (lightweight)

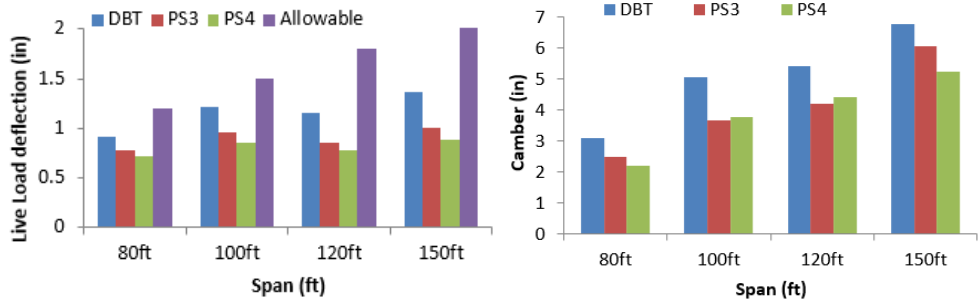
Span	Type	Span to depth ratio	Concrete material (kip/ft/6 ft)		No. of strands	
			Composite = Non Composite		No.	Ratio (PS/DBT)
			Weight (kips)	Ratio (PS/ DBT)		
80'	DBT	27.43	0.68	1.00	18	1.00
	PS3	27.43	0.70	1.03	17	0.94
	PS4	27.43	0.76	1.12	15	0.83
100'	DBT	28.57	0.71	1.00	24	1.00
	PS3	28.57	0.76	1.15	25	1.04
	PS4	28.57	0.82	1.15	21	0.88
120'	DBT	27.17	0.78	1.00	26	1.00
	PS3	27.17	0.88	1.21	27	1.04
	PS4	27.17	0.94	1.21	23	0.88
150'	DBT	27.69	0.83	1.00	30	1.00
	PS3	27.69	1.00	1.20	34	1.13
	PS4	27.69	1.06	1.28	28	0.93

Live load deflection and camber

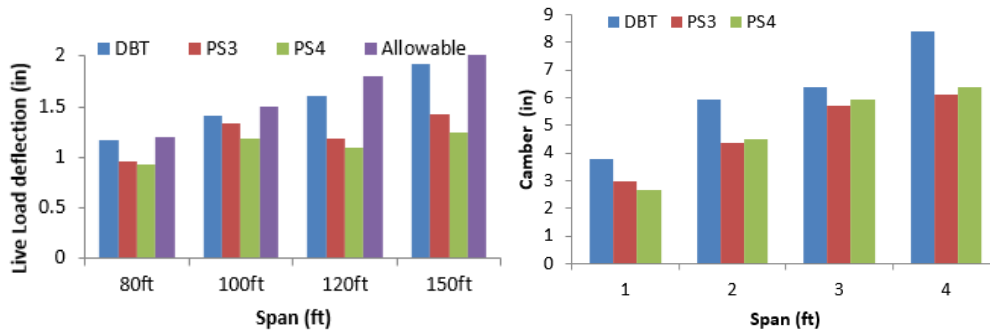
Figure 28 illustrates the live load deflection and camber for all un-topped systems. PS4 features the lowest live load deflection for both normal weight and lightweight concrete options. This suggests that the additional weight present in PS4 creates a stiffer system. PS3 is generally ranked second in terms of providing lower live load deflections and camber. The proposed systems provide lower cambers compared to the traditional decked bulb tee system. Lower camber is desired with respect to reducing the magnitude of positive restraint moments due to creep in bridges made continuous for live loads. If positive restraint moments are too large they may cause cracking in the continuity diaphragm and affect the continuity of the bridge for live loads. Table 19 provides a summary of live load deflections and camber for all un-topped systems and shows that the proposed systems are stiffer than the traditional decked bulb tee system. Again, these results suggest that the proposed systems can be used competitively with the traditional decked bulb tee system especially in cases when live load deflection and camber is a concern. In all cases the live load deflection was smaller than the allowable deflection based on AASHTO provisions, which was calculated as the span length divided by 800.

When lightweight concrete was used live load deflections and camber were higher compared to the normal weight concrete option. Because the overall depth of the superstructure was kept the same for all investigated systems for a given span, the reduction in material stiffness provided by lightweight concrete resulted in higher live load deflections and camber.

Camber in the proposed un-topped systems was higher than the camber in the proposed topped systems for cases when the depth of superstructure for a given span was similar. For example for the 80 ft and 100 ft spans the depth of PS1 and PS2 is 33 in., and 39 in., respectively. Whereas the depth of PS3 and PS4 is 35 in., and 41 in., respectively. An examination of camber values for these two cases reveals that the camber in the topped systems is much lower than that in the un-topped systems. The difference in depth and number of strands is clearly expected to cause a difference in camber values. In addition, the eccentricity between the center of strands and the centroid of the precast section is larger in the un-topped systems compared to the topped systems. This results in higher cambers for the un-topped systems.



Normal weight concrete



Lightweight concrete

Figure 28

Live load deflection and camber comparison (un-topped system)

Table 19
Live load deflections and camber for un-topped systems

Parameter	Span (ft)	NW				LW			
		DBT (in.)	PS3 (in.)	PS4 (in.)	Smallest	DBT (in.)	PS3 (in.)	PS4 (in.)	Smallest
Live load Deflection	80	0.91	0.78	0.72	PS4	1.17	0.96	0.93	PS4
	100	1.22	0.96	0.86	PS4	1.41	1.33	1.19	PS4
	120	1.15	0.85	0.78	PS4	1.60	1.19	1.09	PS4
	150	1.37	1.01	0.89	PS4	1.92	1.42	1.24	PS4
Camber	80	3.09	2.48	2.19	PS4	3.78	2.97	2.66	PS4
	100	5.05	3.67	3.79	PS3	5.92	4.37	4.50	PS3
	120	5.42	4.22	4.42	PS3	6.39	5.72	5.91	PS3
	150	6.79	6.08	5.24	PS4	8.39	6.13	6.38	PS3

Shallower depths

The next step was to determine how much shallower could the superstructure depth be for the traditional system if LLDFs for moment computed from FEA were used instead of those calculated based on AASHTO LFRD Specifications [8]. During this exercise the deflection check was omitted provided that it is not mandatory, and all bridges were checked for

stresses at service and strength at ultimate load levels. Table 20 provides superstructure depths for the decked bulb tee system for various spans. The typical superstructure depth was obtained from the PCI Bridge Design Manual and the shallowest superstructure depth was determined by designing the superstructure according to AASHTO LRFD Specifications using computed LLDFs for moment [12], [8]. The results in Table 20 suggest that the utilization of lower LLDFs computed from finite element analyses results in shallower superstructure depths for the traditional decked bulb tee system. The difference in heights varies from 3 in. to 6 in. The use of lightweight concrete results in slightly shallower superstructure depth but in general the shallowest superstructure depths for normal weight and lightweight concrete option for the decked bulb tee system are similar. Accordingly, when the depth of the superstructure is of concern, a more refined analysis in terms of LLDFs can result in a shallower superstructure and can help the designer meet the vertical clearance requirements present at the site.

Table 20
Superstructure depths for DBT system

Superstructure System	Span (ft)	Typical height* (in.)	Shallowest height** NW (in.)	Shallowest height** LW (in.)
DBT	80	35	32	31
	100	41	37	37
	120	53	48	47
	150	65	61	60

*Obtained from PCI Bridge Design Manual, **Designed based on computed LLDFs

Once the shallowest superstructure depth for the traditional system was obtained, the proposed systems were designed to maintain the same depth and a comparison in terms of weight and the number of strands required was performed. Because PS4 was more competitive than PS3 with the decked bulb tee system the number of strands required for the reduced superstructure depth was calculated only for PS4. Table 21 shows the weight and the number of strands required for the decked bulb tee and PS4 systems when the reduced depth is used. The weight of PS4 system is still slightly larger than the weight of the decked bulb tee system. However, the number of strands required for the PS4 systems is less than that required for the decked bulb tee system. This continues to demonstrate the competitive use of the proposed PS4 system.

Table 21
Number of strands for PS4 and shallowest DBT

Span (ft)	NW					LW				
	Height (in.)	Weight (k/ft)		No. of strands		Height (in.)	Weight (k/ft)		No. of strands	
		DBT	PS4	DBT	PS 4		DBT	PS4	DBT	PS 4
80	32	0.84	0.91	22	19	31	0.66	0.72	22	17
100	37	0.87	0.98	32	27	37	0.69	0.78	28	23
120	48	0.94	1.11	32	30	47	0.75	0.88	30	26
150	61	1.02	1.28	36	35	60	0.81	1.01	34	30

The final exercise in terms of comparison was to determine whether the proposed systems could supply a shallower superstructure depth compared to the absolute minimum obtained for the traditional systems. The superstructure depth for the proposed systems was made 2 in. shallower than the absolute minimum for the traditional systems and the required number of strands was determined. It was outside the scope of work to determine the absolute minimum superstructure depth for a given span for the proposed systems because the main goal was to demonstrate that the proposed systems are competitive with the traditional systems. The weight of the PS4 system for the reduced depth is still slightly larger than the deeper decked bulb tee system but the required number of strands continuous to be less than that required for the decked bub tee system despite the shallower depth. The 2 in. reduction in depth results in slightly lighter precast beams for the PS4 system.

Table 22
Number of strands required for PS4 system for shallower superstructure depths

Span (ft)	NW			LW		
	Height (in.)	Weight (k/ft)	No. of strands - PS4	Height (in.)	Weight (k/ft)	No. of strands - PS4
80	30	0.89	20	29	0.70	18
100	35	0.95	28	35	0.76	25
120	46	1.09	30	45	0.86	27
150	59	1.25	36	58	0.99	31

Longitudinal Connections

Topped Systems

Tensile forces in the connections along the longitudinal joints in the proposed topped systems were quantified with the purpose of estimating the load demand in each connection. The tensile force in each connection was calculated by recording the transverse normal stress in each finite element present in the bottom precast flange for a longitudinal distance of 12 in.,

which represents the connection length with the adjacent member. This stress was then multiplied by the total projected area of the finite elements present in the region described above. The magnitude of transverse tensile forces varied from 5.40 kips to 5.76 kips for PS1 and from 5.76 kips to 6.12 kips for PS2. The span length did not appear to create a marked difference. The tensile forces in each connection were smaller in PS2.

Table 23
Transverse tensile forces in PS1

PS1	Span length (ft)		
	80	100	120
Stress (ksi)	0.15	0.15	0.16
Area in tension (in ²)	36	36	36
Tension (kips)	5.40	5.40	5.76

Spacing of connections = 4 ft

Table 24
Transverse tensile forces in PS2

PS2	Span length (ft)		
	80	100	120
Tensile Stress (ksi)	0.16	0.17	0.17
Area in tension (in ²)	36	36	36
Tension force (kip)	5.76	6.12	6.12

Spacing of connections = 4 ft

The tensile force demands on the proposed UHPC connection were compared with tested capacities on similar connections provided by Halbe [15]. Halbe performed several beam splice tests using UHPC fill as part of an investigation to develop alternative connections for adjacent box beam bridges [15]. The beam splice test setup is shown in Figure 29, and the splice detail is shown in Figure 30. The goal of the investigation was to determine whether the rebar splice shown in Figure 30 can fully develop the yield strength of the bars when the pocket is filled with UHPC. This connection detail is very similar to the the UHPC connection proposed for the topped systems. Table 25 illustrates the test matrix for the beam splice tests and highlights the cases that are similar to the proposed UHPC connection. The splice length in the proposed UHPC connection is 5 in. if a 1.0 in. cover is provided from the end of the field installed bar and the face of the pocket. This is identical with the highlighted splice length in Table 25. The length of the pocket in the proposed connection is 12 in, which is greater than the 11 in. pocket length highlighted in Table 25. The fill material is proposed to be UHPC and the design compressive strength of precast beams is 8 ksi. Both of these

match with what was used in the highlighted tests. The only differences are that the pocket depth in the tested configuration is 5 in. as opposed to 3 in. proposed for the topped systems. Also, the width of the pocket used in the tests is 10 in. as opposed to 12 in. proposed for the topped systems. However, a wider pocket width is expected to improve performance.

If the transverse bars are fully developed and 2-No.4 bars are used then the capacity provided is:

$$T_{\text{yieldbars}} = 2 \times A_s \times f_y = 2 \times 0.2 \text{ in}^2 \times 60 \text{ ksi} = 24 \text{ kips} > 6.12 \text{ kips}^*$$

*(Maximum tension force computed from FEA for the topped systems)

If 2-No.6 bars are used and they are fully developed then the provided capacity is:

$$T_{\text{yieldbars}} = 2 \times A_s \times f_y = 2 \times 0.44 \text{ in}^2 \times 60 \text{ ksi} = 52.8 \text{ kips} > 6.12 \text{ kips}^*$$

*(Maximum tension force computed from FEA for the topped systems)

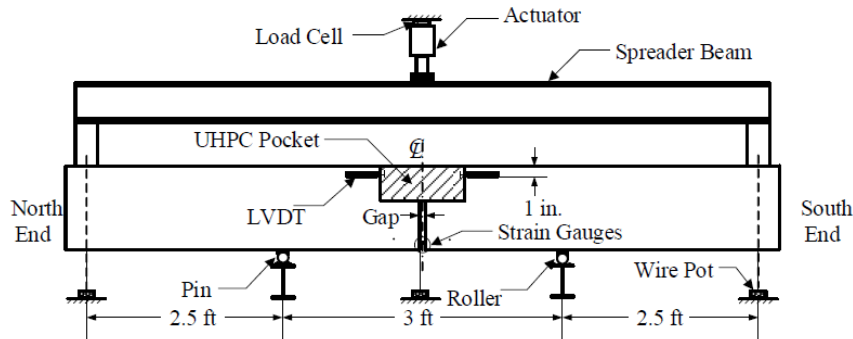


Figure 29
Test setup for beam splice tests (reprinted from Halbe [15])

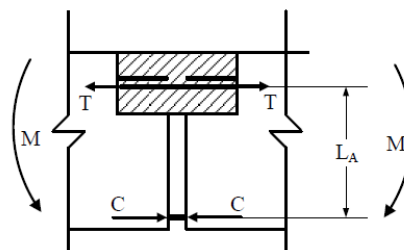


Figure 30
Splice detail and force diagram (reprinted from Halbe [15])

Table 25
Test matrix for beam splice tests (adapted from Halbe [15])

Specimen Designation	Tension Steel	Splice Length (in.)	Pocket Length (in.)	Pocket Filler	Compression Steel	Concrete Strength (ksi)	
U-4-5-I-E	2 No. 4s	5	11	UHPC	2 No.4s	8	
U-4-6-I-E		6	13				
U-4-3-I		3	7				
U-4-4-I		4	9				
U-4-5-II		5	11				
U-4-5-I		2 No. 8s	5	11	VHPC	2 No. 8s	5
U-4-6-I			6	13		2 No. 8s	5
U-4-5-II			5	15		2 No. 8s	5
U-4-3-I			3	17		2 No. 8s	5
U-4-4-I			4	21		2 No. 8s	5
U-4-4-II	4		9	2 No. 8s		5	
U-6-5-I-E	2 No. 6s		5	11		UHPC	2 No.6s
U-6-6-I-E		6	13				
U-6-7-I		7	15	2 No.8s and 1 No.7	5		
U-6-8-I		8	17				

The actuator load required to yield the tension steel in the beam splice tests is 12.8 kips for the 2-No.4 bars, and 28.2 kips for the 2-No.6 bars (Halbe [15]). Table 26 and Table 27 suggest that the maximum actuator load recorded during the tests was always greater than the load required to yield the tension steel in the beam splice tests. This suggests that the tested splice configuration is capable of developing the full yield strength of the bars. Also, the first cracking load was either slightly under the maximum tension force demand (8.64 kips) for the proposed topped systems or above it. However, Halbe states that the first crack generally occurred in the precast beam in the region above the roller supports and not in the vicinity of the UHPC pocket [15]. Again, because of the difference in the pocket depth, 5 in. in the tested configuration versus 3 in. in the proposed configuration, the proposed configuration needs to be tested to ensure adequate capacity during service and ultimate loads. However, the large margin between the required capacity and the tested capacity suggest that the proposed connection configuration should meet load demands.

Table 26
Results of beam splice tests with 2-No.4 tension bars (adapted from Halbe [15])

Specimen Designation	Splice Length (in.)	Compression Reinforcement	First cracking load (lbs)	Maximum load (lbs)	Failure Mode
U-4-5-I-E	5	2 No.4s	7200	28,000	-
U-4-6-I-E	6	2 No.4s	6900	26,500	-
U-4-3-I	3	2 No.7s and 1 No. 6	5800	15,700	slip
U-4-4-I	4	2 No.7s and 1 No. 6	7500	24,500	slip/split
U-4-5-II	5	2 No.7s and 1 No. 6	9000	29,600	slip/split
V-4-5-I	5	2 No. 8	3,200	24,500	slip/split
V-4-6-I	6	2 No. 8	3,000	28,700	slip/split
V-4-5-II	5	2 No. 8	1,500	28,300	rupture
V-4-3-I	3	2 No. 8	1,000	21,300	slip/split
V-4-4-I	4	2 No. 8	2,000	21,800	slip
V-4-4-II	4	2 No. 8	1,500	23,800	slip/split

Table 27
Results of beam splice tests with 2-No.6 tension bars (adapted from Halbe [15])

Specimen Designation	Splice Length (in.)	Compression Reinforcement	First Cracking Load (lb.)	Maximum Load (lb.)	Failure Mode
U-6-5-I-E	5	2 No.6s	7800	35,080	slip
U-6-6-I-E	6	2 No.6s	8000	35,710	slip
U-6-7-I	7	2 No.8s and 1 No.7	9000	43,200	slip/split
U-6-8-I	8	2 No.8s and 1 No.7	9300	43,480	slip/split

The second proposed connection for the topped systems is a welded configuration. A similar connection configuration was tested by Menkulasi as part of a study to develop a new bridge system for short to medium span bridges with spans ranging from 20 ft to 60 ft [16]. A partial transverse cross-section of the developed bridge configuration is shown in Figure 31 and the tested welded connection is shown in Figure 32. Figure 33 shows the test setup used to investigate the effects of transverse bending in the bridge system in question and Figure 34 illustrates the tested specimens that featured welded connections. Specimen capacities were predicted using strut and tie models (Figure 35) and the predicted capacities were compared to those obtained experimentally. Tie capacities were obtained by multiplying the area of the welded bars with the tested ultimate stress and the number of bars.

Table 23 illustrates the characteristics of the tested specimens and highlights the ones that are similar with the proposed welded connection configuration for the topped systems. While the illustrated tested connection detail is similar to the one proposed for the topped bridge

systems there are some differences that need to be noted. The thickness of the precast flange in the tested connection was 3 in., whereas the thickness of the precast flange in the proposed topped systems is 6 in. The length of the steel plate in the tested connection is 6 in., whereas the length of the plate in the proposed connection for the topped system is 12 in. There are a total of two bars welded to the back of the inclined steel plate in the tested connection, whereas the number of welded bars in the proposed connection is four.

Intuitively the tested configuration should provide approximately half the capacity of the proposed configuration for the topped systems. Given that the predicted capacities for the tested connections were based on the measured ultimate stress and given that the predicted capacities were either similar to the tested capacities or lower for the welded connections, it can be deduced that the capacity of the proposed connection can be based on the yield strength of the welded bars provided that connection at the back of the plate features a complete penetration weld. If the capacity of the proposed connection were to be based on the yield strength of the bars assuming that No. 6 bars are used, then the provided capacity is as follows:

$$T_{\text{yieldbars}} = A_s \times f_y = 0.44 \text{ in}^2 * 4 \text{ (number of bars)} * 60 \text{ ksi} = 105.6 \text{ kips} \gg 6.12 \text{ kips}^*$$

*(Maximum tension force computed from FEA for the topped systems)

If we assume four No.4 bars then the predicted capacity is as follows:

$$T_{\text{yieldbars}} = A_s \times f_y = 0.2 \text{ in}^2 * 4 \text{ (number of bars)} * 60 \text{ ksi} = 48 \text{ kips} \gg 6.12 \text{ kips}^*$$

*(Maximum tension force computed from FEA for the topped systems)

These results suggest that the proposed connection configuration should be able to resist the applied tensile forces at service and ultimate levels.

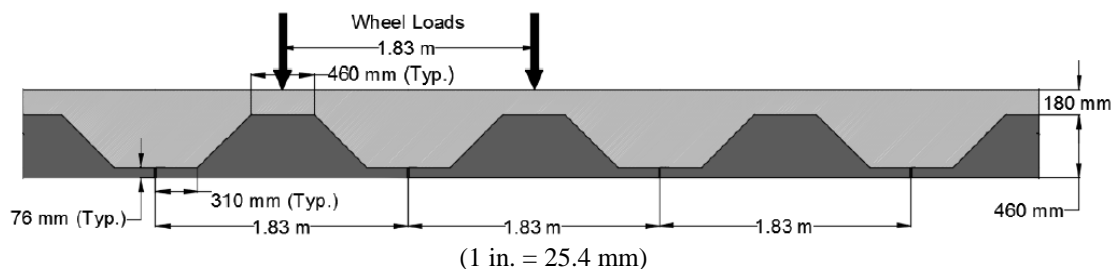


Figure 31
Partial transverse cross-section of the bridge system developed by Menkulasi [16]

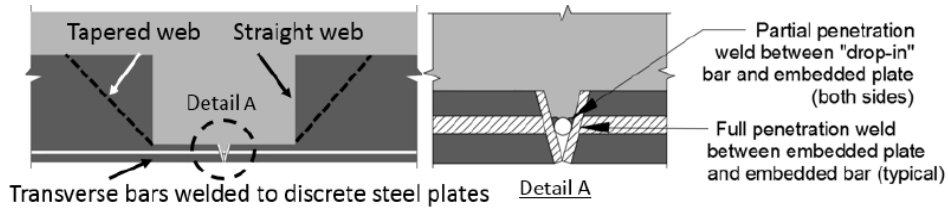


Figure 32
Welded connection tested by Menkulasi [16]

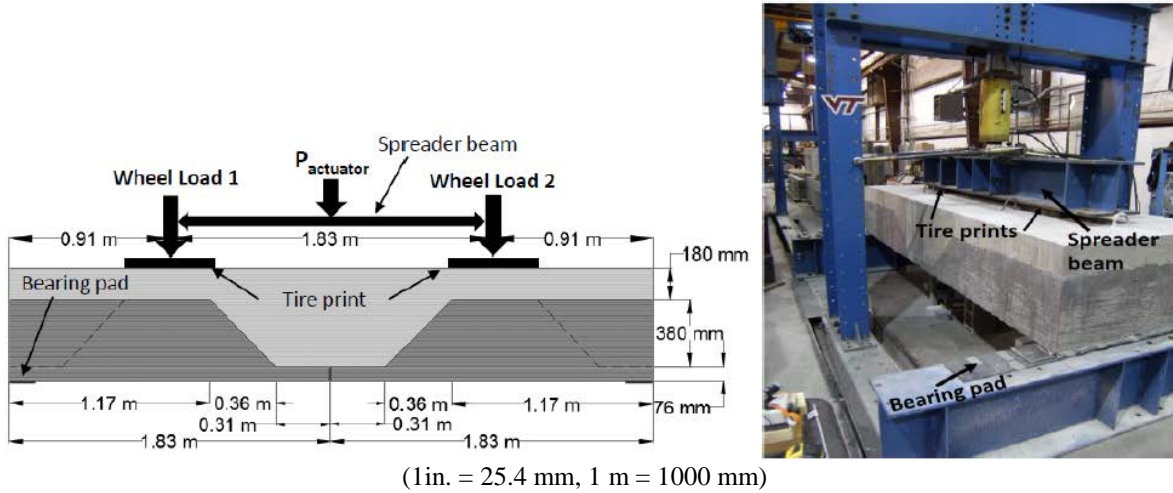


Figure 33
Test setup used by Menkulasi [16]

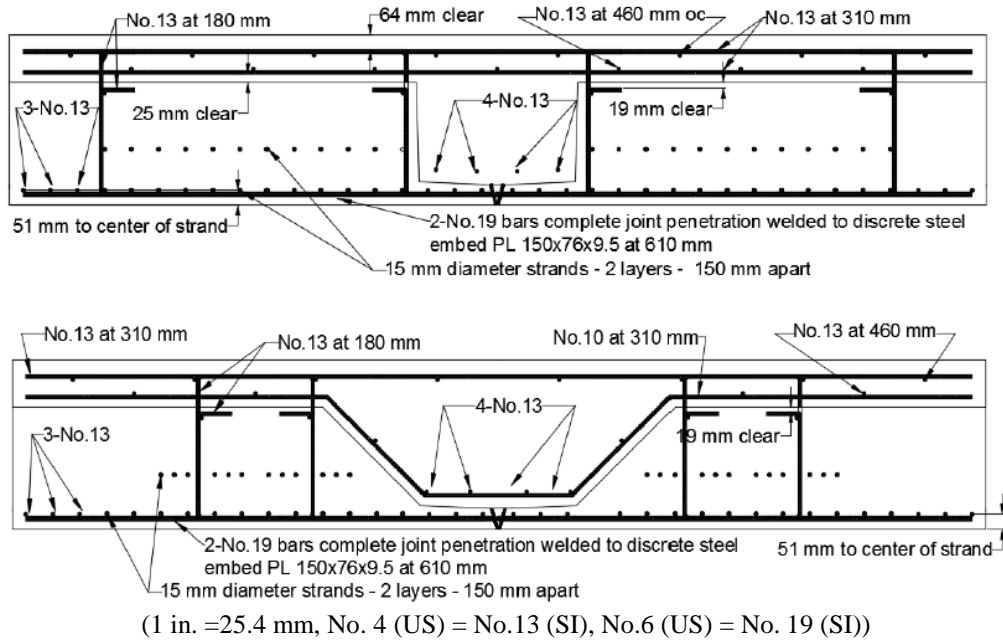


Figure 34
Tested specimens with welded connections (Menkulasi [16])

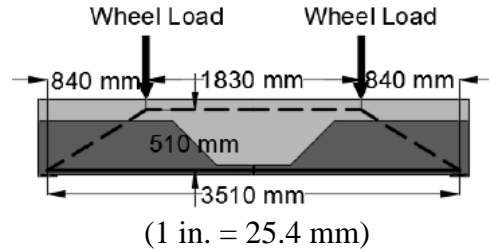


Figure 35
Strut and tie model (Menkulasi [16])

Table 28
Test matrix for specimens tested during Phase I (Menkulasi [16])

Specimen ID	Cross-sectional shape	Connection	Transverse bottom reinforcing in CIP trough	Transverse bottom reinforcing in precast	Loading
Trial	Straight web	Extended bars	No. 19 at 310 mm plus No.13 stirrups at 310 mm	No. 19 at 310 mm hooked bars plus No. 10 stirrups at 460 mm	¼ point
1	Straight web	Extended bars	No. 19 at 310 mm plus No. 13 at 310 mm	No. 19 at 310 mm hooked bars plus No. 10 stirrups at 460 mm	¼ point
2	Straight web	Embedded plate and welded rebar	None	4 – No. 19 bars	¼ point
3	Tapered web	Embedded plate and welded rebar	No. 10 at 310 mm	4 – No. 19 bars	¼ point
4	Tapered web	No connection	No.19 at 310 in.	No. 10 at 460 mm	¼ point

(1 in. = 25.4 mm, No.3 (US) = No.10 (SI), No. 4 (US) = No.13 (SI), No.6 (US) = No. 19 (SI))

Table 29
Test results for specimens tested by Menkulasi [16]

Phase	Specimen ID	P _{crtest} (kN)	P _{utest} (kN)	P _{upredicted} ^a (kN)	FS _{cr}	FS _{ultimate}	Ratio= P _{upredicted} /P _{utest}
I	Trial	356	1335 ^b	1068	2.27	7.48	0.80
I	1	401	1157 ^c	1068	2.50	6.53	0.92
I	2	445	1001 ^d	1078	2.74	5.70	1.08
I	3	490	1335 ^b	1078	2.98	7.48	0.81
I	4	267	401 ^e	361	1.80	2.50	0.90
II	5	312	1068 ^f	1078	2.00	6.00	1.01
II	6	312	623 ^g	980	2.00	3.70	1.57
II	7	223	361 ^h	485	2.00	3.10	1.34

^a Predicted actuator load to cause failure. Prediction was based on strut and tie models

^b Test stopped due to capacity of loading frame

^c Many cracks in CIP topping in all directions

^d Fracture of weld at one location and rebar at another

^e Large crack through precast section

^f Large crack in CIP topping above joint

^g Large crack in CIP topping above joint and parallel with the tapered interface on one side

^h Large crack at the precast CIP interface and through CIP topping

(1 kip = 4.448 kN)

Un-topped Systems

The transverse bending positive moments in un-topped systems were quantified so that the spacing of the U-shaped bars could be determined accordingly. Because the connection along the longitudinal joint is a continuous connection, transverse bending moments were quantified for every foot of length. The top precast flange was modeled with two layers of finite elements. The calculation of the transverse bending moments was done by multiplying the tension and compression forces in the top precast flange with the moment arm between them. The tensile force was calculated by recording the transverse normal tensile stress in the bottom layer of finite elements in the top precast flange and by multiplying it with the projected area of these finite elements. The stress was calculated at the centroid of the finite element it was taken equal to the average centroidal stress of the finite elements in the most critical one foot strip. It should be noted that the magnitude of the transverse tensile stress reduced significantly in regions away from the wheel load. The compression force was calculated similarly. The tensile force was then multiplied with the moment arm between the tensile force and compression force present in the finite elements towards the top of the precast flange.

Transverse bending moments varied from 21.60 k-in/ft to 23.76 k-in/ft for PS3 and from 28.08 k-in/ft to 32.40 k-in/ft for PS4. The maximum positive moment in the connection computed from the finite element models was either smaller or similar to that computed

using AASHTO's strip method described earlier. For example, the maximum positive moment at the longitudinal connection computed from the finite element model for PS3 was 23.76 in-kips/ft, whereas that calculated using AASHTO's strip method was 37.31 in-kips/ft. As a result, AASHTO's strip method can be used to conservatively design the top precast flange in the transverse direction as well as to estimate the moment demand along the longitudinal joint. For PS4, the maximum transverse positive bending moment along the connection computed from the finite element model was 32.4 in-kips/ft, whereas that calculated using AASHTO's strip method was 28.36 in-kips/ft. AASHTO's method results in a slightly lower moment (12% lower), however considering that the transverse moment computed from the model was obtained in the worst one foot strip and that the magnitude of it reduces significantly away from the most critical region, it is reasonable to use AASHTO's strip method for design purposes. It should be noted that the effective strip width calculated based on AASHTO was approximately 66 in.

Transverse bending moments were also calculated for the traditional DBT system and varied from 47.52 kip-in/ft to 50.76 k-in/ft. The transverse bending moment demand at the longitudinal connections at service for the proposed un-topped systems is less than 2/3 of the maximum computed for the decked bulb tee system. This is due to the fact that the cantilever length for the precast flange in the deck bulb tee system is larger than that in the proposed un-topped systems. Accordingly, the utilization of PS4 reduces the transverse bending moment demand on longitudinal connections in addition to offering shallower superstructure depths.

The cracking moment for the 6 in. precast flange in the transverse direction is 48.2 in-kip/ft if gross cross-sectional properties are used, and 52.09 in-kips/ft if the un-cracked transformed cross-sectional properties are used. This indicates that no cracking should be expected in the region around the longitudinal connection in all investigated un-topped systems provided that the strength of the closure pour matches that of the precast concrete beam flange. Accordingly, it is recommended that the design compressive strength of the closure pour when the bridge is opened to traffic is at least $f'_c=8,000$ psi.

Table 30
Transverse bending moment in PS3

PS3	80 ft	100 ft	120ft	150 ft
Tensile stress (ksi)	0.22	0.20	0.21	0.20
Area in tension (in ² /ft)	36	36	36	36
Tension force (kips/ft)	7.92	7.20	7.56	7.20
Moment arm (in.)	3	3	3	3
Moment (kip-in/ft)	23.76	21.60	22.68	21.60

Continuous longitudinal connection

Table 31
Transverse bending moment in PS4

PS4	80 ft	100 ft	120ft	150 ft
Tensile stress (ksi)	0.28	0.30	0.26	0.27
Area (in ² /ft)	36	36	36	36
Tension force (kips/ft)	10.08	10.80	9.36	9.72
Moment arm (in.)	3	3	3	3
Moment (kip-in/ft)	30.24	32.40	28.08	29.16

Continuous longitudinal connection

Table 32
Transverse bending moment in DBT

DBT	80 ft	100 ft	120ft	150 ft
Tensile stress (ksi)	0.44	0.46	0.47	0.46
Area (in ² /ft)	36	36	36	36
Tension force (kips/ft)	15.84	16.56	16.92	16.56
Moment arm (in.)	3	3	3	3
Moment (kip-in/ft)	47.52	49.68	50.76	49.68

Continuous longitudinal connection

The transverse bending moment demands for the proposed un-topped systems were compared with bending moment capacities of a similar connection detail tested by French et al. as part of an NCHRP project to develop connection details for decked bulb tee systems that emulate continuity and monolithic action [7]. The slab panels and shear key details tested by French et al. are shown in Figure 36 [7]. The joint reinforcing details are shown in Figure 37. The overall depth of the deck panels is 6.25 in. as opposed to 6 in. which is the precast top flange thickness for the proposed un-topped systems. Two types of closure pour materials were included in deck panel testing. The first is the Set 45 formulation, which requires an overnight cure, and the second is a high performance concrete mix which,

requires a seven day cure. Both of these closure pour materials were included in static and fatigue testing. Table 33 shows which closure pour material was used in which type of test. The tested concrete compressive strengths for the precast deck panels and closure pour materials are summarized in Table 34. The tested compressive strengths for the deck panels were always higher than the specified 7 ksi strength and also higher than the 8 ksi strength used in the development of the un-topped systems. The lowest compressive strength for the closure pour material was 4592 psi at the start of the test. The yield stress of the U-shaped steel bars was 75 ksi and the type of steel was deformed wire. French et al. noted that stainless steel is also an alternative [7]. It should be noted that a higher grade steel or other type of steel may not achieve the minimum bent diameter required to provide the specified clearances. The test specimens were labeled using the following designation:

S = static or shear

F = fatigue or flexure

O = overnight cure

7 = seven day cure

For example the test specimen labeled SS-O is a deck panel tested in a static mode in which the applied load created shear in the joint in addition to flexure and the applied closure pour material required an overnight cure.

Table 35 shows the measured deck panel moment capacities. The lowest measured deck panel moment capacity is 19.34 ft-kip/ft (232.08 in-kip/ft). This is much larger than the transverse moment at service computed in this study for the proposed un-topped systems, which is 63.72 in-kips/ft. Although the depth of the tested deck panels was 0.25 in. larger than the precast flange thickness in the proposed systems, such a small reduction in thickness (4%) is not expected to significantly affect the transverse bending moment capacity of the connection. Additionally, the spacing of the U-bars (4.5 in.) may be increased provided that the supplied capacity will not be mobilized.

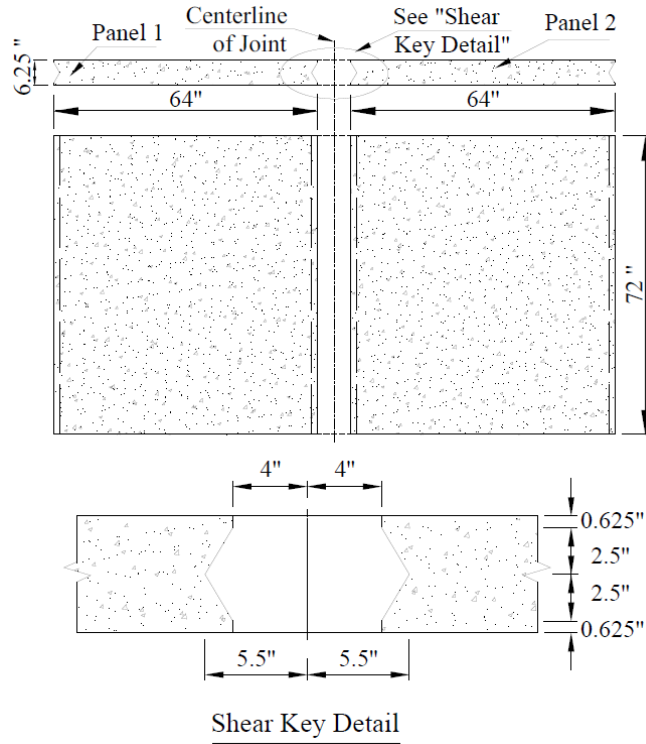


Figure 36
Tested slab dimensions and shear key details (French et al. [7])

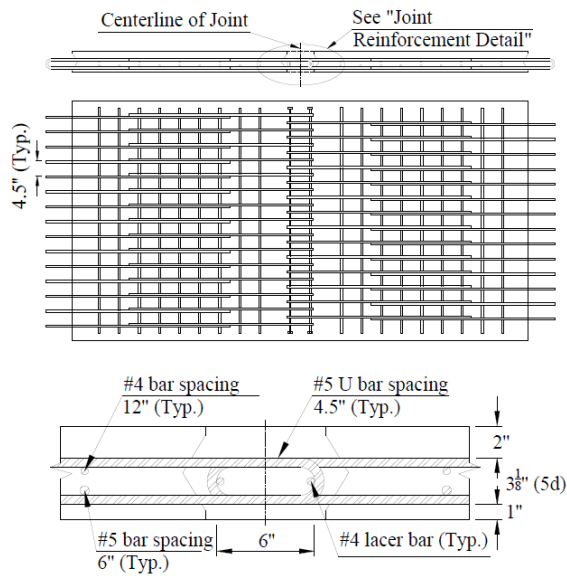


Figure 37
Joint reinforcing details (French et al. [7])

Table 33
Closure pour materials used by French et al. [7]

Overnight Cure				7 day Cure			
Flexure		Flexure-Shear		Flexure		Flexure-Shear	
Static	Fatigue	Static	Fatigue	Static	Fatigue	Static	Fatigue
Set 45 HW extended	Set 45 HW	Set 45 HW	Set 45 HW extended	HPC Mix 1			

Table 34
Tested concrete compressive strengths (French et al. [7])

Specimen	Panel (psi)		Joint (psi)	
	Start of test	End of test	Start of test	End of test
SS-O	11512*		7586	
SS-7	11512*		8740	
FS-O	10687	11512*	6321	6572
FS-7	11512*	11512*	7861	9417**
SF-O	12441		5939	
SF-7	12441		6966	
FF-O	11711	11632	4592	5345
FF-7	11035	11711	10796***	12361

*The panels for FS-O, FS-7, SS-O, and SS-7 were fabricated with the same batch of concrete and were tested or the test was finished more than 120 days after the panels were fabricated. The 148-day concrete compressive strength of 11,512 psi is the reported strength.

**The test FS-7 started 5 days after the joint was cast, and finished 13 days after the joint was cast. The strength reported here is the 21-day joint strength.

***The FF-7 test started at the age of 22 days, and the joint strength reported in the table is the 8-day strength.

Table 35
Measured panel moment capacities (French et al. [7])

Specimen	Measured		
	Panel Compressive Strength (f'_c) (psi)	Joint Compressive Strength (f'_c) (psi)	Failure Load (kip-ft/ft)
SS-O	11512	7586	19.34
FS-O	11512	6572	22.18
SS-7	11512	8740	25.44
FS-7	11512	9417	23.30
SF-O	12441	5939	24.21
FF-O	11632	5345	19.39
SF-7	12441	6966	31.5*
FF-7	11711	12361	31.5*

*SF-7 and FF-7 specimens were beyond the MTS capacity (31.5 kip-ft/ft) and couldn't be failed by MTS

CONCLUSIONS

A total of four composite concrete bridge systems were developed for short and medium span bridges with spans ranging from 80 ft to 150 ft. These bridge systems are lightweight, efficient in flexure and shear and can be used in sites with stringent vertical clearance requirements while being able to accelerate construction. The developed systems consist of adjacent hollow precast concrete beams with and without concrete topping. The topped systems were compared with the traditional adjacent box beam system and the un-topped systems were compared with the traditional decked bulb tee system. Both normal weight and lightweight options were investigated. The comparison was made in terms of span to depth ratios, weight, number of strands, live load deflection and camber.

It was demonstrated that both of the proposed topped systems (PS1 and PS2) are lighter than the traditional adjacent box system. Additionally, PS2 requires fewer strands than the traditional system for a given depth and exhibits lower camber. PS2 also offers shallower superstructure depths for a given span compared to the adjacent box system. This is a significant advantage when it comes to meeting vertical clearance requirements at a given site. Both proposed topped systems address the reflective cracking problems manifested in adjacent box beam systems by shifting the location of the longitudinal connections towards the bottom and away from the traffic loads. Such a shift in the location of longitudinal connections is intended to emulate monolithic action without the need for transverse post-tensioning. It was shown that lower live load distribution factors could be obtained when a more refined analysis is performed compared to those calculated using AASHTO provisions [8]. The use of these lower LLDFs for moment led to the selection of shallower superstructure depths. Therefore in cases when vertical clearance requirements are stringent the use of a more refined analysis to obtain live load distribution factors can lead to a design that complies with the geometrical limitations on the site.

The proposed un-topped systems are slightly heavier than the traditional decked bulb tee system, however they require a smaller number of strands for a given depth. Additionally, the live load deflection and camber for PS3 and PS4 is generally less than that for the traditional decked bulb tee system. PS4 also offers shallower superstructure depths for a given span, which is advantageous in sites with stringent vertical clearance requirements. It was demonstrated that computed LLDFs for moment were lower than those calculated based on AASHTO provisions for decked bulb tee systems [8]. The use of lower LLDFs for moment led to shallower superstructure depth even for the traditional decked bulb tee system. Therefore the use a more refined analysis to obtain LLDFs for moment is one option when

trying to meet stringent vertical clearance requirements at a specific site.

PS2 and PS4 appear to be more competitive than PS1 and PS3. LLDFs, for PS1/PS2 and PS3/PS4 can be conservatively estimated using AASHTO provisions for adjacent box and decked bulb tee systems, respectively, [8].

For all proposed systems the forces applied to the longitudinal connections were quantified in terms of transverse tensile forces and transverse bending moments. Various longitudinal connections details were proposed. The force demands for the proposed connections were compared with tested capacities of similar configurations and it was concluded that the proposed connections provide a viable solution to create continuity between adjacent precast members. Physical testing will need to be done specifically for the proposed connection to ensure satisfactory performance during service and ultimate load levels. In the proposed untopped systems transverse bending moment demands on the longitudinal connections and on the top precast flange are reduced due to the reduced span provided by the two web supports as opposed to the single web support in the decked bulb tee system.

ACRONYMS, ABBREVIATIONS, AND SYMBOLS

AASHTO	American Association of State Highway and Transportation Officials
cm	centimeter(s)
DBT	Decked Bulb Tee
d_b	Bar diameter
FEA	Finite element analysis
FHWA	Federal Highway Administration
ft.	foot (feet)
in.	inch(es)
kN	kiloNewton(s)
LADOTD	Louisiana Department of Transportation and Development
LLDF	Live load distribution factor
LTRC	Louisiana Transportation Research Center
lb.	pound(s)
m	meter(s)
mm	millimeter(s)
PS1	Proposed system 1
PS2	Proposed system 2
PS3	Proposed system 3
PS4	Proposed system 4
Typ.	Typical

REFERENCES

1. Kamel, M. R., Tadros, M. K. (1996). The Inverted Tee Shallow Bridge System for Rural Areas. *PCI journal*, 41(5), 28-43.
2. Huckelbridge Jr, A. A., El-Esnawi, H., Moses, F. (1995). "Shear key performance in multibeam box girder bridges", *J. Perf. Constr. Facil.*, 9(4), 271-285.
3. Miller, R. A., Hlavacs, G. M., Long, T., Greuel, A. (1999). "Full-scale testing of shear keys for adjacent box girder bridges", *PCI J.*, 44(6), 80-90.
4. El-Remaily. A., Tadros, M.K., Yamane, T., Krause, G., (1996). "Transverse Design of Adjacent Precast Prestressed Concrete Box Girder Bridges", *PCI J.*, July-August, 96-113.
5. Badwan, I., Liang, R. Y. (2007). "Transverse post-tensioning design of precast concrete multibeam deck", *PCI Journal*, 52(4), 84-92.
6. Hanna, K. E., Morcous, G., Tadros, M. K. (2009). "Transverse post-tensioning design and detailing of precast, prestressed concrete adjacent-box-girder bridges", *PCI J.* 54(4), 160-174.
7. French. C.W., Shield, C.K., Klasesus, D. Smith, M., Eriksson, W., Ma, J.Z., Zhu, P., Lewis, S., Chapman, C.E. (2011). "Cast-in-Place Concrete Connections for Precast Deck Systems." NCHRP Web-Only Document 173, Washington, DC, January.
8. AASHTO (2013) "LRFD Bridge Design Specifications", 6th Edition, Washington, DC.
9. Mathcad 14, PTC, Needham, MA.
10. Leap Conspan, Bentley Systems Incorporated, Exton, PA.
11. Abaqus User's Manual Version 6.14-2, Dassault Systemes Simulia Corp. (2014).
12. Precast Prestressed Concrete Institute, (2003) "Precast Prestressed Concrete Bridge Design Manual," Chicago, IL.
13. <http://altusprecast.com/products/c-grid/> (Accessed February 2015)
14. Gordon, S. R.; May, I. M., (2005) "Development of In Situ Joints for Pre-Cast Bridge Deck Units," *Bridge Engineering* 000, Issue BEO, pp. 1-14.
15. Halbe, K., (2014) "New approach to connections between members of adjacent box beam bridges", PhD Dissertation, Department of Civil and Environmental Engineering, Virginia Tech, Blacksburg, VA.
16. Menkulasi, F., (2014) "The Development of a Composite Concrete Bridge System for Short-to-Medium-Span Bridges", PhD Dissertation, Department of Civil and Environmental Engineering, Virginia Tech, Blacksburg, VA.